

QCD sum rules for quark-gluon three-body components in the B meson

Tetsuo NISHIKAWA*

Faculty of Health Science, Ryotokuji University, Urayasu, Chiba 279-8567, Japan

Kazuhiro TANAKA†

*Department of Physics, Juntendo University, Inzai, Chiba 270-1695, Japan
and J-PARC Branch, KEK Theory Center, Institute of Particle and Nuclear Studies,
High Energy Accelerator Research Organization (KEK),
203-1, Shirakata, Tokai, Ibaraki, 319-1106, Japan*

(Dated: September 29, 2018)

We discuss the QCD sum rule calculation of the heavy-quark effective theory parameters, λ_E and λ_H , which correspond to matrix elements representing quark-gluon three-body components in the B -meson wavefunction. We derive the sum rules for $\lambda_{E,H}$ calculating the new higher-order QCD corrections, i.e., the order α_s radiative corrections to the Wilson coefficients associated with the dimension-5 quark-gluon mixed condensates, and the power corrections due to the dimension-6 vacuum condensates. We find that the new radiative corrections significantly improve the stability of the corresponding Borel sum rules and lead to the reduction of the values of $\lambda_{E,H}$. We also discuss the renormalization-group improvement for the sum rules and present update on the values of $\lambda_{E,H}$.

I. INTRODUCTION

The B mesons play distinguished roles in exploring CP violation and the flavor sector of the Standard Model. In particular, the measurements of the B -meson decays can provide precise information on the relevant quark couplings [1]. Since the properties of those decays are also influenced by the complicated strong-interaction effects responsible for forming the B -meson, as well as the final-state hadrons, a better theoretical control of the nonperturbative effects inside the B mesons is now becoming very important. This is also interesting in its own right as understanding the properties of the simplest meson including a heavy quark.

In the heavy-quark limit based on $\Lambda_{\text{QCD}}/m_B \ll 1$, $\Lambda_{\text{QCD}}/m_b \ll 1$ with m_B and m_b being the masses of the B -meson and b -quark, the matrix elements using a B -meson state obey heavy-quark symmetry, and are conveniently described by the heavy-quark effective theory (HQET) [2]. In this framework, fundamental properties of the B mesons are represented by the HQET parameters that are defined as matrix elements of the relevant local operators, like the decay constant F [2]:

$$\langle 0 | \bar{q} \gamma_\rho \gamma_5 h_v | \bar{B}(v) \rangle = iF(\mu) v_\rho. \quad (1)$$

Here, $|\bar{B}(v)\rangle$ is the \bar{B} -meson state with the 4-velocity v in the HQET, \bar{q} is the light-antiquark field, h_v is the effective heavy-quark field, and the heavy-light local operator in the LHS is renormalized at the scale μ . The decay constant of Eq.(1) represents the quantitative content of the quark-antiquark valence component inside the B meson in the heavy-quark limit, so that $F(\mu)$ determines the normalization of the valence Fock components in the B -meson wavefunction, as well as of the amplitude for the exclusive B -meson decays. We note that $F(\mu)$ is related to the physical decay constant f_B as

$$f_B \sqrt{m_B} = F(\mu) \left[1 + \frac{C_F \alpha_s}{4\pi} \left(3 \ln \frac{m_b}{\mu} - 2 \right) + \dots \right] + O(1/m_b), \quad (2)$$

with the corresponding short-distance coefficient shown in the parentheses to the one-loop accuracy, as well as with the $O(1/m_b)$ correction terms in the heavy-quark expansion. The value of f_B is now obtained rather precisely from lattice QCD calculations as [3] (see also [4, 5])

$$f_B = 0.195 \pm 0.013 \text{ GeV}, \quad (3)$$

*Electronic address: nishikawa@ryotokuji-u.ac.jp

†Electronic address: kztanaka@juntendo.ac.jp

which is consistent [6] with the results of measurement of the branching fraction for $B \rightarrow \tau \nu$ decays in the Belle [7] and Babar [8] experiments.

We can also define the analogues of Eq.(1), which are associated with the higher Fock components inside the B meson. For the non-minimal parton configurations with additional gluons, the corresponding HQET parameters were introduced by Grozin and Neubert [9] as

$$\langle 0 | \bar{q} \alpha \cdot g \mathbf{E} \gamma_5 h_v | \bar{B}(v) \rangle = F(\mu) \lambda_E^2(\mu), \quad (4)$$

$$\langle 0 | \bar{q} \sigma \cdot g \mathbf{H} \gamma_5 h_v | \bar{B}(v) \rangle = i F(\mu) \lambda_H^2(\mu), \quad (5)$$

in terms of the matrix elements in the B -meson rest frame with $v = (1, \mathbf{0})$. Here, the three-body quark-gluon operators are associated with the chromoelectric and chromomagnetic fields, $E^i = G^{0i}$ and $H^i = (-1/2)\epsilon^{ijk}G^{jk}$, with $G_{\mu\nu} = G_{\mu\nu}^a T^a$ and $G_{\mu\nu}^a = \partial_\mu A_\nu^a - \partial_\nu A_\mu^a + gf^{abc}A_\mu^b A_\nu^c$ being the gluon field strength tensor. The values of $\lambda_{E,H}^2$ were also estimated in [9] using QCD sum rules, as

$$\begin{aligned} \lambda_E^2(\mu) &= 0.11 \pm 0.06 \text{ GeV}^2, \\ \lambda_H^2(\mu) &= 0.18 \pm 0.07 \text{ GeV}^2, \end{aligned} \quad (6)$$

at $\mu = 1 \text{ GeV}$. Besides this rather rough estimate, there exists no other estimate at present. In this paper, we present an extension of Grozin-Neubert's QCD sum rule calculation of $\lambda_{E,H}^2$, taking into account the higher-order perturbative and nonperturbative effects in QCD. The main new ingredient in the present case is that we calculate the relevant QCD radiative corrections, so that we derive our sum rules to the order α_s accuracy. We find that, only after including those new contributions, the perturbative as well as nonperturbative corrections to the sum rules for $\lambda_{E,H}^2$ become under control. We note that, also for the QCD sum-rule calculations of the decay constant (1), the order α_s radiative corrections produce the large and essential contributions to yield the values consistent with Eq.(3) [2, 10, 11].

One might anticipate that the higher Fock components in the B meson would give rise to the “higher-twist” power corrections to the hard exclusive amplitudes, similarly as the roles played by the higher Fock components in the light mesons π , ρ , etc. [12], and thus the impact of a more accurate determination of $\lambda_{E,H}^2$ than Eq.(6) would be marginal. Actually, however, it has been revealed that the behaviors of the contributions induced by the higher Fock components are quite different between the B -meson case and the light-meson case: the presence of a heavy quark inside the B -meson causes the nonperturbative quark-gluon interactions which induce the mixing of the effects corresponding to the different twist [9, 13, 14]. In particular, recently, it has been demonstrated that the B -meson “light-cone distribution amplitudes” to describe the valence Fock components participating in the hard exclusive processes [9, 13–17] are contaminated by the multiparticle Fock states, so that the contributions represented by the novel HQET parameters $\lambda_{E,H}^2$ of Eqs. (4), (5) could strongly affect [18] the amplitudes for the exclusive B -meson decays at the *leading* power. Indeed, the normalization of the so-called hard spectator interaction amplitude [1] could be modified by a factor two or more, when varying the values of $\lambda_{E,H}^2$ in the uncertainty range of Eq.(6) [18]. Therefore, an improved estimate of $\lambda_{E,H}^2$ is desirable to have a better control of the hadronic uncertainty associated with the B meson, which is a major source of theoretical uncertainty in the calculations of the decay rates [1, 19].

The paper is organized as follows. Section II is mainly introductory; we set up a systematic formalism for the QCD sum rule calculation of $\lambda_{E,H}^2$ in the HQET, as well as the decay constant F , and apply it to reproduce the previous results for the sum rules of those HQET parameters. We explain that the previous sum-rule estimate of $\lambda_{E,H}^2$ needs update including higher-order effects. In Sec. III, we derive the new power corrections to the sum rules for $\lambda_{E,H}^2$, due to the nonperturbative QCD condensates. Section IV is devoted to the calculation of the new order α_s corrections to the sum rules for $\lambda_{E,H}^2$. Taking into account all these new contributions, we present the final form of our sum rules for $\lambda_{E,H}^2$ in Sec. V. We explain the renormalization-group improvement of our sum rule formulas and perform their detailed numerical analysis to obtain a new estimate of $\lambda_{E,H}^2$. We find that the new values of $\lambda_{E,H}^2$ are significantly modified from those of Eq.(6). Section VI is reserved for conclusions.

II. QCD SUM RULES IN THE HQET

In this section we set up the framework convenient for treating the perturbative as well as nonperturbative corrections to the suitable correlation functions in the HQET for the QCD sum-rule calculations of the B -meson matrix elements λ_E and λ_H , and also use it to demonstrate that the calculation of the leading effects reproduces the sum rules obtained previously by Grozin and Neubert [9]. The complete treatment including the new perturbative and nonperturbative corrections is presented in the succeeding sections.

We consider the following correlation functions in the HQET (the dependence on the renormalization scale μ is suppressed for simplicity):

$$\begin{aligned} & i \int d^4x e^{-i\omega v \cdot x} \langle 0 | T [\bar{q}(0) \Gamma_1 h_v(0) \bar{h}_v(x) \Gamma_2 q(x)] | 0 \rangle \\ & = -\frac{1}{2} \text{Tr} [\Gamma_1 P_+ \Gamma_2] \Pi_F(\omega), \end{aligned} \quad (7)$$

$$\begin{aligned} & i \int d^4x e^{-i\omega v \cdot x} \langle 0 | T [\bar{q}(0) \Gamma_1 g G_{\mu\nu}(0) h_v(0) \bar{h}_v(x) \Gamma_2 q(x)] | 0 \rangle \\ & = -\frac{1}{2} \text{Tr} [\sigma_{\mu\nu} \Gamma_1 P_+ \Gamma_2] \Pi_{3H}(\omega) \\ & \quad - \frac{1}{2} \text{Tr} [(iv_\mu \gamma_\nu - iv_\nu \gamma_\mu) \Gamma_1 P_+ \Gamma_2] \Pi_{3S}(\omega), \end{aligned} \quad (8)$$

where $P_+ = (1 + \not{v})/2$ is the projector on the upper components of the heavy-quark spinor, Γ_1 is an arbitrary gamma matrix, and we choose $\Gamma_2 = \gamma_5$ to construct the sum rules for pseudoscalar B meson. (The case for the vector meson B^* can also be treated by choosing $\Gamma_2 = \gamma_\mu - v_\mu$ and yields exactly the same results as in the pseudoscalar B -meson case due to heavy-quark spin symmetry in the HQET.) Eq. (7) is the familiar correlator between two heavy-light currents and the correlation function $\Pi_F(\omega)$ provides the sum rules to evaluate the decay constant F . On the other hand, the correlator (8) between the two-body current and the three-body current involving the gluon field strength tensor defines the correlation functions, $\Pi_{3H}(\omega)$ and $\Pi_{3S}(\omega)$, corresponding to the two independent Lorentz structures; as we will show shortly, $\Pi_{3H}(\omega)$ and $\Pi_{3S}(\omega)$ allow us to derive the sum rules to evaluate λ_H^2 and the “splitting” $\lambda_H^2 - \lambda_E^2$, respectively (see Eqs. (4), (5)).

In the general procedure of QCD sum rules, we evaluate the above correlation functions by the operator product expansion (OPE) in the unphysical region $-\omega \gg \Lambda_{\text{QCD}}$ on one hand and express those correlation functions in terms of the properties (masses and matrix elements) associated with the physical states participating in the spectra at $\omega > 0$ on the other hand; we relate these two descriptions exploiting the analyticity properties of the correlation functions, which are embodied by the corresponding dispersion relations. The dispersion relation satisfied by $\Pi_F(\omega)$ of Eq. (7) is well-known, and the dispersion relations of similar type are obeyed also by $\Pi_{3H}(\omega)$ and $\Pi_{3S}(\omega)$ of (8); namely, for $X = F, 3H, 3S$,

$$\Pi_X(\omega) = \frac{1}{\pi} \int_0^\infty d\omega' \frac{\text{Im} \Pi_X(\omega')}{\omega' - \omega - i0}, \quad (9)$$

up to the appropriate subtraction terms that are polynomial in ω . Indeed, these relations can be demonstrated by inserting a complete set of states between the two currents in the corresponding correlators: the LHS of Eq. (7) yields (in the B -meson rest frame)

$$\begin{aligned} & \frac{1}{2(\bar{\Lambda} - \omega - i0)} \langle 0 | \bar{q}(0) \Gamma_1 h_v(0) | \bar{B}(v) \rangle \\ & \quad \times \langle \bar{B}(v) | \bar{h}_v(0) \Gamma_2 q(0) | 0 \rangle + \dots, \end{aligned} \quad (10)$$

and the LHS of Eq. (8) gives the similar result with Γ_1 replaced by $\Gamma_1 g G_{\mu\nu}(0)$. Here, a pole arises at $\bar{\Lambda} = m_B - m_b$, the usual effective mass of the B meson, accompanying the matrix elements that are parameterized by the corresponding HQET parameters (renormalized at the scale μ) as

$$\langle 0 | \bar{q}(0) \Gamma_1 h_v(0) | \bar{B}(v) \rangle = -\frac{i}{2} F(\mu) \text{Tr} [\Gamma_1 P_+ \gamma_5], \quad (11)$$

$$\begin{aligned} & \langle 0 | \bar{q}(0) \Gamma_1 g G_{\mu\nu}(0) h_v(0) | \bar{B}(v) \rangle \\ & = -\frac{i}{6} F(\mu) \left\{ \lambda_H^2(\mu) \text{Tr} [\Gamma_1 P_+ \gamma_5 \sigma_{\mu\nu}] \right. \\ & \quad \left. + [\lambda_H^2(\mu) - \lambda_E^2(\mu)] \text{Tr} [\Gamma_1 P_+ \gamma_5 (iv_\mu \gamma_\nu - iv_\nu \gamma_\mu)] \right\}, \end{aligned} \quad (12)$$

and the ellipses stand for the similar pole contributions of higher resonances and the continuum contributions. Combining the results with Eqs. (7), (8), one finds,

$$\Pi_F(\omega) = \frac{F^2(\mu)}{2} \frac{1}{\bar{\Lambda} - \omega - i0} + \dots,$$

$$\begin{aligned}\Pi_{3H}(\omega) &= \frac{F^2(\mu)}{6} \lambda_H^2(\mu) \frac{1}{\bar{\Lambda} - \omega - i0} + \cdots, \\ \Pi_{3S}(\omega) &= \frac{F^2(\mu)}{6} [\lambda_H^2(\mu) - \lambda_E^2(\mu)] \frac{1}{\bar{\Lambda} - \omega - i0} + \cdots,\end{aligned}\quad (13)$$

which hold in any frame as well as in the rest frame, and show that the contribution of the B meson to the spectral functions in Eq. (9) is completely expressed by the relevant HQET parameters. Calculating the LHS of Eqs. (7), (8) based on the OPE and matching the results with the formulas in Eq.(13), we obtain the sum rules associated with those HQET parameters.

We follow the standard procedure to construct the corresponding QCD sum rules: we apply the Borel-transformation operator, defined by

$$\hat{B}_M \equiv \lim_{\substack{n \rightarrow \infty, -\omega \rightarrow \infty \\ M = -\omega/n \text{ fixed}}} \frac{\omega^n}{\Gamma(n)} \left(-\frac{d}{d\omega} \right)^n, \quad (14)$$

to the relevant correlation functions obeying the dispersion relation (9), (13). This transformation introduces the Borel parameter M instead of the external energy ω as

$$\hat{B}_M \Pi_X(\omega) = \frac{1}{M} \int_0^\infty d\omega' e^{-\omega'/M} \frac{1}{\pi} \text{Im} \Pi_X(\omega'), \quad (15)$$

and eliminates the subtraction terms. Eq.(14) implies that the power-correction terms associated with the higher dimensional operators in the OPE are factorially ($\sim 1/n!$) suppressed, improving the convergence of the series and, simultaneously, Eq.(15) indicates that the contributions of higher resonances and continuum are exponentially suppressed compared with that of the lowest-lying state, minimizing the dependence on the contributions of the excited states. Employing quark-hadron duality, we approximate, as usual, those excited-state contributions to the spectral function in Eq.(15) by the continuum contribution which is based on the OPE result and starts from the ‘‘continuum threshold’’ ω_{th} ; namely, we use

$$\begin{aligned}\frac{1}{\pi} \text{Im} \Pi_F(\omega) &= \frac{1}{2} F^2(\mu) \delta(\omega - \bar{\Lambda}) \\ &+ \frac{1}{\pi} \text{Im} \Pi_F^{\text{OPE}}(\omega) \theta(\omega - \omega_{\text{th}}),\end{aligned}\quad (16)$$

with the correlation function $\Pi_F^{\text{OPE}}(\omega)$ calculated in the OPE, and the similar form for $(1/\pi) \text{Im} \Pi_X(\omega)$ ($X = 3H, 3S$) with the corresponding OPE result, $\Pi_X^{\text{OPE}}(\omega)$. Then, we obtain the sum rules,

$$F^2(\mu) e^{-\bar{\Lambda}/M} = 2 \int_0^{\omega_{\text{th}}} d\omega e^{-\omega/M} \frac{1}{\pi} \text{Im} \Pi_F^{\text{OPE}}(\omega), \quad (17)$$

$$F^2(\mu) \lambda_H^2(\mu) e^{-\bar{\Lambda}/M} = 6 \int_0^{\omega_{\text{th}}} d\omega e^{-\omega/M} \frac{1}{\pi} \text{Im} \Pi_{3H}^{\text{OPE}}(\omega), \quad (18)$$

$$\begin{aligned}F^2(\mu) [\lambda_H^2(\mu) - \lambda_E^2(\mu)] e^{-\bar{\Lambda}/M} \\ = 6 \int_0^{\omega_{\text{th}}} d\omega e^{-\omega/M} \frac{1}{\pi} \text{Im} \Pi_{3S}^{\text{OPE}}(\omega),\end{aligned}\quad (19)$$

and, taking the ratios of Eqs. (18) and (19) with Eq.(17) to cancel the factor $F^2(\mu)$, one can evaluate $\lambda_H^2(\mu)$ and $\lambda_H^2(\mu) - \lambda_E^2(\mu)$, respectively, based on the sum rules.

Now the remaining task is to calculate $\Pi_X^{\text{OPE}}(\omega)$, to be substituted into the RHS of Eqs. (17)-(19). Carrying out the OPE of the corresponding correlation functions for the region $-\omega \gg \Lambda_{\text{QCD}}$, the results generically take the form,

$$\begin{aligned}\Pi_X^{\text{OPE}}(\omega) &= C_I^X(\omega) + C_q^X(\omega) \langle \bar{q}q \rangle + C_G^X(\omega) \langle G^2 \rangle \\ &+ C_\sigma^X(\omega) \langle \bar{q}gG \cdot \sigma q \rangle + \cdots,\end{aligned}\quad (20)$$

with $X = F, 3H, 3S$, where $\langle \bar{q}q \rangle \equiv \langle 0 | \bar{q}q | 0 \rangle$, $\langle G^2 \rangle \equiv \langle 0 | (G_{\mu\nu}^a)^2 | 0 \rangle$, and $\langle \bar{q}gG \cdot \sigma q \rangle \equiv \langle 0 | \bar{q}gG^{\mu\nu} \sigma_{\mu\nu} q | 0 \rangle$ are the quark condensate, the gluon condensate, and the quark-gluon-mixed condensate, respectively, as the vacuum expectation values of the dimension-3, -4, and -5 local operators, and are associated with the corresponding Wilson coefficients $C_k^X(\omega)$ with $k = q, G$, and σ ; an increase in dimension of the operators implies extra powers of $1/\omega$ for the corresponding Wilson coefficients, and the ellipses in Eq.(20) denote the terms with the operators of dimension $d \geq 6$. $C_I^X(\omega)$,

associated with the unit operator, coincides with the purely perturbative contribution to $\Pi_X(\omega)$. The condensates as well as the coefficient functions in general depend on the renormalization scale μ .

For the correlation function (7) with the two-body currents, the OPE can be derived in a standard way and the Wilson coefficients appearing in Eq.(20) with $X = F$ are obtained [10, 11, 20, 21, 28] by evaluating the familiar Feynman diagrams, which involve the heavy-quark propagator in a background gluon field A_μ ,

$$\underbrace{h_v(0)\bar{h}_v(x)} = \theta(-v \cdot x)\delta^{(D-1)}(x_\perp)P_+ \times \mathcal{P} \exp \left(ig \int_{v \cdot x}^0 ds v \cdot A(sv) \right), \quad (21)$$

for the case of the D dimensions, where $x_\perp^\mu = x^\mu - (v \cdot x)v^\mu$, and the factor in the second line, i.e., the straight Wilson line along the velocity v with the path-ordering operator \mathcal{P} , allows us to organize the interactions with the gluon field A_μ exactly in the HQET. Thus, it is convenient to use the Fock-Schwinger gauge, $x^\mu A_\mu(x) = 0$, for the background gluon field, so that the heavy quark does not interact with the nonperturbative gluons in the calculation for power corrections to the correlation function (7) (see Fig. 2(a) below). In this case, it is also well-known that we have very useful relations [22]: for the classical background gluon field,

$$A_\mu(x) = \int_0^1 du u x^\nu G_{\nu\mu}(ux), \quad (22)$$

and, for the light-quark propagator,

$$\underbrace{q(x)\bar{q}(0)} = \frac{i\Gamma\left(\frac{D}{2}\right)\not{x}}{2\pi^{\frac{D}{2}}(-x^2+i0)^{\frac{D}{2}}} + \frac{i\Gamma\left(\frac{D}{2}-1\right)}{32\pi^{\frac{D}{2}}(-x^2+i0)^{\frac{D}{2}-1}}\{\not{x}, \sigma^{\mu\nu}\}gG_{\mu\nu}(0) + \dots, \quad (23)$$

with the ellipses denoting the terms associated with operators of dimension $d \geq 3$; it is worth noting that the term associated with the dimension-4 operator G^2 is absent from the ellipses. We do not give the details of the calculation of the Wilson coefficients here but, for later convenience, sketch the relevant steps: we decompose the quark as well as gluon fields into the “quantum” and “classical” parts; the quantum parts are contracted to yield the propagators in the classical background fields, like Eqs. (21), (23), while the classical parts satisfy the classical equations of motion, $\not{D}q = 0$, $v \cdot Dh_v = 0$, and $D^\nu G_{\mu\nu}^a = g \sum_{q'} \bar{q}' \gamma_\mu T^a q'$ with the summation over all quark flavors. For the matching at the leading accuracy in α_s , the correlator in the LHS of Eq.(7) is evaluated as

$$T [\bar{q}(0)\Gamma_1 h_v(0) \bar{h}_v(x)\Gamma_2 q(x)] = \underbrace{\bar{q}(0)\Gamma_1 h_v(0)\bar{h}_v(x)\Gamma_2 q(x)} + \underbrace{\bar{q}(0)\Gamma_1 h_v(0)\bar{h}_v(x)\Gamma_2 q(x)}, \quad (24)$$

and, substituting Eqs. (21)-(23) into the first term in the RHS, we immediately obtain C_I^F in Eq.(20) as the purely perturbative contribution and also find that C_G^F vanishes up to the corrections of $O(\alpha_s^2)$, as a direct consequence of the absence of the operator G^2 in Eq.(23) as noted above. On the other hand, the vacuum expectation value of the second term in the RHS of Eq.(24) yields,

$$\begin{aligned} & \theta(-v \cdot x)\delta^{(3)}(x_\perp) \langle 0 | \bar{q}(0)\Gamma_1 P_+ \Gamma_2 q(x) | 0 \rangle, \\ & = \theta(-v \cdot x)\delta^{(3)}(x_\perp) [\langle 0 | \bar{q}(0)\Gamma_1 P_+ \Gamma_2 q(0) | 0 \rangle \\ & + x^\mu \langle 0 | \bar{q}(0)\Gamma_1 P_+ \Gamma_2 D_\mu q(0) | 0 \rangle \\ & + \frac{1}{2} x^\mu x^\nu \langle 0 | \bar{q}(0)\Gamma_1 P_+ \Gamma_2 D_\mu D_\nu q(0) | 0 \rangle + \dots] \\ & = \theta(-v \cdot x)\delta^{(3)}(x_\perp) \text{Tr} [\Gamma_1 P_+ \Gamma_2] \\ & \times \frac{1}{4} \left[\langle \bar{q}q \rangle + \frac{1}{16} x^2 \langle \bar{q}gG \cdot \sigma q \rangle + \dots \right], \end{aligned} \quad (25)$$

where we used the equations of motion $\not{D}q = 0$ in the last equality, and this allows us to obtain C_q^F as well as C_σ^F . As the result, the relevant Wilson coefficients read [10, 20, 21]

$$C_I^F(\omega) = -\frac{N_c}{2\pi^2} \omega^2 \ln \frac{-\omega}{\mu},$$

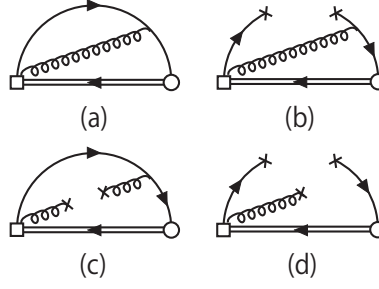


FIG. 1: Nonvanishing diagrams for the OPE of the correlation function (8) in the Fock-Schwinger gauge. The double line denotes the propagator of the effective heavy quark, and the circle and box represent the two- and three-body currents, respectively. The four diagrams (a)-(d) generate, respectively, the first four terms of (20) with $X = 3H, 3S$.

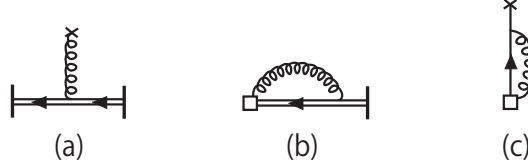


FIG. 2: The vanishing subdiagrams. (a) is associated with classical background gluon field of Eq.(22). (b) and (c) have a loop involving quantum gluon field emanating from the field strength tensor in the three-body current. The external lines with a bar at their end are amputated.

$$\begin{aligned} C_q^F(\omega) &= \frac{1}{2\omega}, \\ C_G^F(\omega) &= 0, \\ C_\sigma^F(\omega) &= -\frac{1}{16\omega^3}, \end{aligned} \quad (26)$$

up to the terms polynomial in ω . We calculate the discontinuities of Eq.(20) with these coefficients, across the cut along the line $\omega > 0$ in the complex ω plane, and substitute the results into the RHS of Eq.(17). This yields the sum rule,

$$\begin{aligned} F^2(\mu)e^{-\bar{\Lambda}/M} &= \frac{2}{\pi^2} N_c M^3 W^{(2)}\left(\frac{\omega_{\text{th}}}{M}\right) - \langle \bar{q}q \rangle \\ &+ \frac{1}{16M^2} \langle \bar{q}gG \cdot \sigma q \rangle, \end{aligned} \quad (27)$$

where the function,

$$W^{(m)}(x) \equiv 1 - \sum_{k=0}^m \frac{x^k}{k!} e^{-x}, \quad (28)$$

arises from the integral over the duality region, $0 < \omega < \omega_{\text{th}}$, in Eq.(17). This sum rule can be used for a leading estimate of the decay constant $F(\mu)$.

The sum rules for a leading estimate of $\lambda_{E,H}^2$ can be derived similarly. The corresponding calculation was performed by Grozin and Neubert [9] with two particular choices for the gamma matrix Γ_1 of (8), which make the corresponding three-body currents coincide with the chromoelectric and chromomagnetic operators in the LHS of Eqs. (4) and (5). For later convenience and for a cross-check of Grozin-Neubert's result, we here perform the corresponding calculation for arbitrary gamma matrix Γ_1 , and summarize the procedures and the results. The correlator between the two-body and three-body currents in the LHS of Eq.(8) is evaluated as

$$\begin{aligned} &T [\bar{q}(0)\Gamma_1 g G_{\mu\nu}(0) h_v(0) \bar{h}_v(x) \Gamma_2 q(x)] \\ &= \bar{q}(0)\Gamma_1 g G_{\mu\nu}(0) h_v(0) \bar{h}_v(x) \Gamma_2 q(x) \\ &\quad + \bar{q}(0)\Gamma_1 g G_{\mu\nu}(0) h_v(0) \bar{h}_v(x) \Gamma_2 q(x) + \dots \end{aligned} \quad (29)$$

By contrast to the above case leading to the results (26), the extra gluons emanating from the three-body current participate in the present case. Those extra gluons can interact with the light quark and such contributions require the participation of the additional quark-gluon coupling in perturbation theory, so as to form the propagator,

$$\begin{aligned} \underbrace{G_{\mu\nu}^a(0)A_\lambda^b(z)} &= \frac{\Gamma\left(\frac{D}{2}\right)\delta^{ab}}{2\pi^{\frac{D}{2}}(-z^2+i0)^{\frac{D}{2}}}(g_{\nu\lambda}z_\mu - g_{\mu\lambda}z_\nu) \\ &+ \frac{\Gamma\left(\frac{D}{2}-1\right)f^{abc}}{8\pi^{\frac{D}{2}}(-z^2+i0)^{\frac{D}{2}-1}}(gG_{\mu\rho}^c(0)z^\rho g_{\nu\lambda} - 2gG_{\mu\lambda}^c(0)z_\nu \\ &- gG_{\nu\rho}^c(0)z^\rho g_{\mu\lambda} + 2gG_{\nu\lambda}^c(0)z_\mu) + \cdots, \end{aligned} \quad (30)$$

for the case of the D dimensions and using the Feynman gauge for the quantum part of the gluon field, with the ellipses denoting the terms associated with operators of dimension $d \geq 3$. The ellipses in Eq.(29) stand for the terms of this type at the leading accuracy in α_s , which are induced by the first term in the RHS of Eq.(30), and the corresponding nonvanishing contributions are represented by the Feynman diagrams (a) and (b) in Fig. 1; note that, by explicit calculation, the subdiagrams (b), (c) in Fig. 2 vanish, reflecting that a physical gluon represented by the field strength tensor does not interact with the heavy quark, nor is absorbed into a single quark on the mass shell. (The contributions induced by the second term of Eq.(30) will be discussed in Sec. IV.) Decomposing those contributions from Figs. 1 (a) and (b) into independent Lorentz structures, as in the RHS of Eq.(8), we obtain the Wilson coefficients C_I^X and C_q^X , respectively, in the OPE (20) with $X = 3H, 3S$.

Similarly, it is straightforward to see that the vacuum expectation value of the first term in the RHS of Eq.(29) yields $C_G^{3H,3S}$, by combining the field strength tensor of the first term of Eq.(29) with that from the second term of the quark propagator (23), corresponding to the diagram (c) in Fig. 1. On the other hand, the contribution of the second term in the RHS of Eq.(29) can be evaluated similarly as Eq.(25), and we obtain,

$$\begin{aligned} &\theta(-v \cdot x)\delta^{(3)}(x_\perp) \langle 0|\bar{q}(0)gG_{\mu\nu}(0)\Gamma_1 P_+ \Gamma_2 q(x)|0\rangle \\ &= \theta(-v \cdot x)\delta^{(3)}(x_\perp) \\ &\quad \times \left(\frac{1}{48} \text{Tr} [\Gamma_1 P_+ \Gamma_2 \sigma_{\mu\nu}] \langle \bar{q}gG \cdot \sigma q \rangle + \cdots \right), \end{aligned} \quad (31)$$

with the term represented by the diagram (d) in Fig. 1 and the ellipses denoting the contributions associated with the operators of dimension $d \geq 6$, so that we can calculate $C_\sigma^{3H,3S}$ using the former contribution. Collecting the results from the diagrams (a)-(d) in Fig.1, we obtain the corresponding Wilson coefficients as

$$\begin{aligned} C_I^{3H}(\omega) &= \frac{1}{18\pi^2} N_c C_F \frac{\alpha_s}{4\pi} \omega^4 \ln \frac{-\omega}{\mu}, \\ C_q^{3H}(\omega) &= C_F \frac{\alpha_s}{2\pi} \omega \ln \frac{-\omega}{\mu}, \\ C_G^{3H}(\omega) &= -\frac{\alpha_s}{24\pi} \ln \frac{-\omega}{\mu}, \\ C_\sigma^{3H}(\omega) &= \frac{1}{24\omega}, \end{aligned} \quad (32)$$

and

$$\begin{aligned} C_I^{3S}(\omega) &= -\frac{1}{18\pi^2} N_c C_F \frac{\alpha_s}{4\pi} \omega^4 \ln \frac{-\omega}{\mu}, \\ C_q^{3S}(\omega) &= C_F \frac{\alpha_s}{2\pi} \omega \ln \frac{-\omega}{\mu}, \\ C_G^{3S}(\omega) &= -\frac{\alpha_s}{24\pi} \ln \frac{-\omega}{\mu}, \\ C_\sigma^{3S}(\omega) &= 0, \end{aligned} \quad (33)$$

up to the terms polynomial in ω , which are irrelevant for the present purpose. Here, $C_F = (N_c^2 - 1)/(2N_c)$, and we note that the dimension-5 mixed condensate does not contribute to Π_{3S}^{OPE} . Substituting (20) with the coefficient

Parameter	Value
$\langle \bar{q}q \rangle$	$(-0.24 \pm 0.02)^3 \text{ GeV}^3$
$\langle \frac{\alpha_s}{\pi} G^2 \rangle$	$(0.012 \pm 0.006) \text{ GeV}^4$
$\langle \bar{q}gG \cdot \sigma q \rangle / \langle \bar{q}q \rangle$	$(0.8 \pm 0.2) \text{ GeV}^2$

TABLE I: Input values of the vacuum condensates at the normalization point $\mu = 1 \text{ GeV}$.

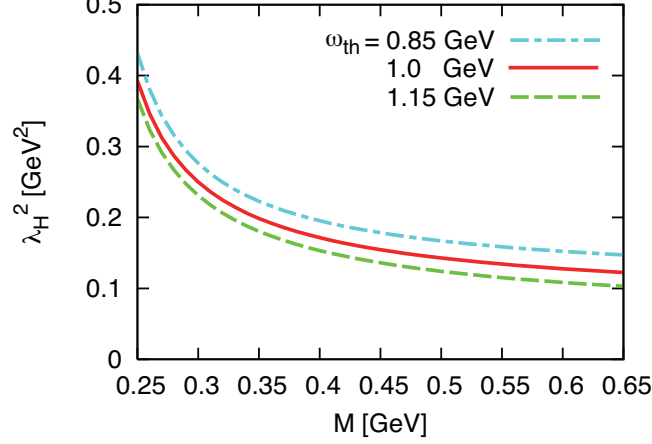


FIG. 3: Borel sum rule for λ_H^2 at $\mu = 1 \text{ GeV}$, using Eq.(34) divided by Eq.(27).

functions (32) and (33) into the RHS of Eqs. (18) and (19), respectively, we obtain

$$\begin{aligned}
 F^2(\mu) \lambda_H^2(\mu) e^{-\bar{\Lambda}/M} = & -\frac{2\alpha_s}{\pi^3} N_c C_F M^5 W^{(4)}\left(\frac{\omega_{\text{th}}}{M}\right) \\
 & -\frac{3\alpha_s}{\pi} C_F M^2 \langle \bar{q}q \rangle W^{(1)}\left(\frac{\omega_{\text{th}}}{M}\right) \\
 & +\frac{M}{4} \langle \frac{\alpha_s}{\pi} G^2 \rangle W^{(0)}\left(\frac{\omega_{\text{th}}}{M}\right) - \frac{1}{4} \langle \bar{q}gG \cdot \sigma q \rangle,
 \end{aligned} \tag{34}$$

and

$$\begin{aligned}
 F^2(\mu) [\lambda_H^2(\mu) - \lambda_E^2(\mu)] e^{-\bar{\Lambda}/M} = & \frac{2\alpha_s}{\pi^3} N_c C_F M^5 W^{(4)}\left(\frac{\omega_{\text{th}}}{M}\right) \\
 & -\frac{3\alpha_s}{\pi} C_F M^2 \langle \bar{q}q \rangle W^{(1)}\left(\frac{\omega_{\text{th}}}{M}\right) \\
 & +\frac{M}{4} \langle \frac{\alpha_s}{\pi} G^2 \rangle W^{(0)}\left(\frac{\omega_{\text{th}}}{M}\right),
 \end{aligned} \tag{35}$$

where, as usual, the factor α_s/π from the coefficient functions $C_G^{3H,3S}$ of Eqs. (32), (33) is combined with the gluon condensate. This set of the sum rules reproduces Grozin-Neubert's sum rule formulas [9] for $\lambda_H^2(\mu)$ and $\lambda_E^2(\mu)$.

In numerical evaluations throughout this paper, we use the standard values for the input parameters collected in Table I. These values have been used in, e.g., a recent QCD sum rule calculation for the B -meson light-cone distribution amplitude [15], and are consistent with the values used in [9]; note that the values of the condensates have been extracted at the $\sim 30\%$ level accuracy [11]. $\alpha_s(1 \text{ GeV}) = 0.4$ was used in [9], but we use the value $\alpha_s(1 \text{ GeV}) = 0.47$ which is consistent with the world average.

In Figs. 3 and 4, we plot $\lambda_H^2(\mu)$ and $\lambda_H^2(\mu) - \lambda_E^2(\mu)$ at $\mu = 1 \text{ GeV}$ as functions of M , obtained by taking the ratios of Eqs.(34) and (35), respectively, with Eq.(27). One finds that the values of λ_H^2 are larger than those of the splitting $\lambda_H^2 - \lambda_E^2$, and, in particular, that the curves for the former show sizeable dependence on the parameter M . Indeed, this considerable variation of λ_H^2 for $0.3 \text{ GeV} \lesssim M \lesssim 0.5 \text{ GeV}$, which was taken in [9] as the “stability window” for the sum rule (27), is responsible for the large errors in Eq.(6). Such poor stability is known to be a common feature to the sum rules for matrix elements of operators with high dimension [12], because the corresponding sum rules are

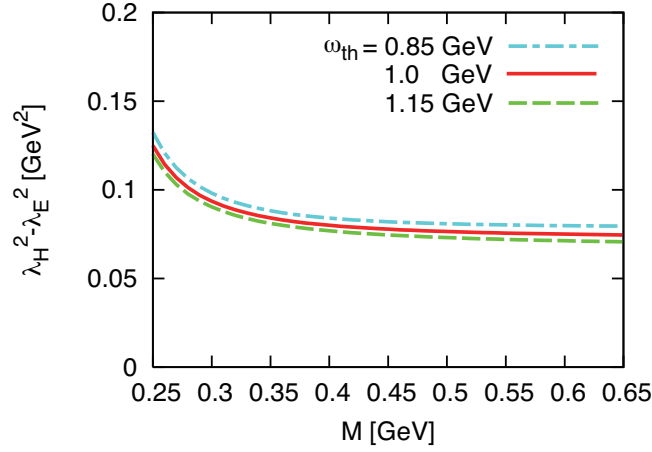


FIG. 4: Borel sum rule for $\lambda_H^2 - \lambda_E^2$ at $\mu = 1$ GeV, using Eq.(35) divided by Eq.(27).

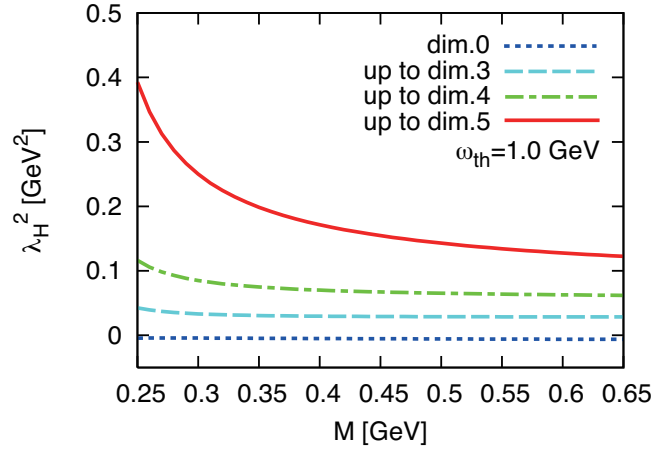


FIG. 5: The separate contributions to the Borel sum rule for λ_H^2 with $\mu = 1$ GeV and $\omega_{th} = 1.0$ GeV, using Eq.(34) divided by Eq.(27). The contributions from each term in the RHS of Eq.(34), organized according to the dimension of the associated operators, are shown.

dominated at small M by the condensates of high dimension. For the present case with the dimension-5 operators in Eqs. (4), (5), the behavior of the sum rule (34) for $0.3 \text{ GeV} \lesssim M \lesssim 0.5 \text{ GeV}$ is mainly determined by the term with the quark-gluon-mixed condensate $\langle \bar{q}gG \cdot \sigma q \rangle$: this is demonstrated in Fig.5, which shows the separate contributions from each term in the RHS of (34), organized according to the dimension of the associated local operators. On the other hand, the term with $\langle \bar{q}gG \cdot \sigma q \rangle$ is absent from the sum rule (35): this sum rule yields a rather stable behavior for $\lambda_H^2 - \lambda_E^2$ as shown in Fig.4, but the separate contributions of each term in the RHS of Eq.(35), shown in Fig.6, indicate that the nonperturbative corrections do not decrease for increasing dimension $d = 0, 3$, and 4 of the associated operators, similarly as in Fig.5. These characteristic behaviors in Figs. 3 and 4 are in contrast to the case of the decay constant, for which the separate contributions to the sum rule (27) are plotted in Fig.7 with the value $\bar{\Lambda} = 0.55 \text{ GeV}$ [9]. These results suggest good convergence of the OPE (20) for $X = F$, with the operators of dimension $d \leq 5$, while the convergence of Eq.(20) for $X = 3H, 3S$, at the same level of accuracy, is questionable. Therefore, we will calculate the nonperturbative corrections to Eq.(20), associated with the dimension-6 operators, and evaluate the corresponding modifications to the sum rules (34) and (35), as well as to Eq. (27), in the next section.

The results for the relevant Wilson coefficients, Eqs. (32) and (33), show that only C_σ^{3H} , associated with the dimension-5 quark-gluon-mixed condensate, is of $O(\alpha_s^0)$, while all the other coefficients are of $O(\alpha_s)$. This is again in contrast to the case of the decay constant, for which all the nonzero coefficients in Eq.(26) are of $O(\alpha_s^0)$. Combined with the behaviors in Figs. 5-7 discussed above, in particular, with those indicating the dominance of the term associated with the dimension-5 operator in Eq.(34), it is desirable to calculate the $O(\alpha_s)$ correction to this term induced by

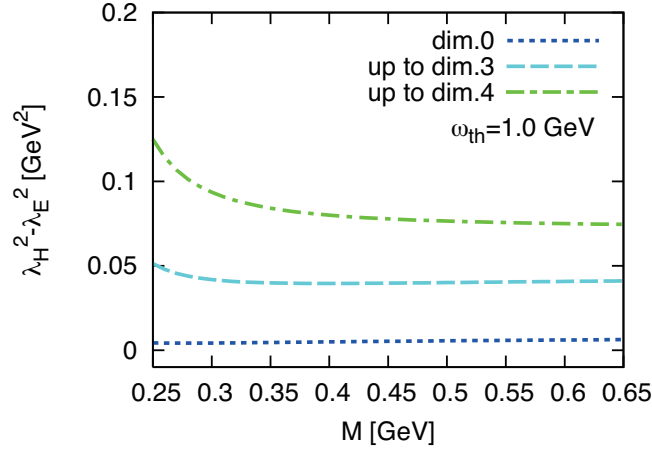


FIG. 6: Same as Fig. 5, but for $\lambda_H^2 - \lambda_E^2$, using Eq.(35) divided by Eq.(27).

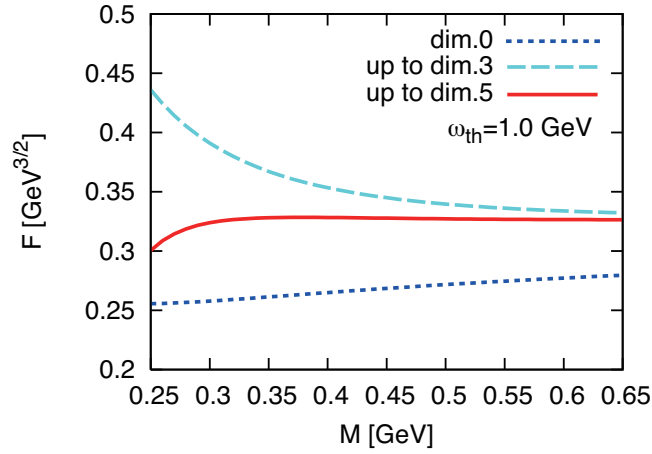


FIG. 7: The separate contributions to the Borel sum rule for F , using Eq.(27) with $\mu = 1$ GeV, $\omega_{\text{th}} = 1.0$ GeV, and $\bar{\Lambda} = 0.55$ GeV. The contributions from each term in the RHS of Eq.(27), organized according to the dimension of the associated operators, are shown.

the next-to-leading order (NLO) correction to the Wilson coefficient C_{σ}^{3H} of Eq.(32). It should be also clarified whether C_{σ}^{3S} of Eq.(33) receive the $O(\alpha_s)$ effects. These new $O(\alpha_s)$ contributions may give the effects comparable with the other $O(\alpha_s)$ contributions displayed in Figs. 5, 6. We will work out the one-loop matching to calculate the corresponding Wilson coefficients at $O(\alpha_s)$ in Sec. IV, and derive the modifications to the sum rules for $\lambda_{E,H}^2$.

III. NONPERTURBATIVE CORRECTIONS WITH DIMENSION-6 OPERATORS

At the leading accuracy in α_s , all the relevant power corrections to Eq.(20) with $X = F$ are generated from the second term in Eq.(24), and the leading contribution in the ellipses in the middle line of Eq.(25) reads

$$\frac{1}{6} x^\mu x^\nu x^\lambda \langle 0 | \bar{q}(0) \Gamma_1 P_+ \Gamma_2 D_\mu D_\nu D_\lambda q(0) | 0 \rangle, \quad (36)$$

which determines the power correction associated with the dimension-6 operator. We exploit the following exact relation between matrix elements of the local operators (Γ is arbitrary gamma matrix) [23],

$$\begin{aligned} \langle 0 | \bar{q} \Gamma D_\mu D_\nu D_\lambda q | 0 \rangle &= \frac{ig^2}{576} \langle 0 | \bar{q} \gamma_\kappa T^a q \sum_{q'} \bar{q}' \gamma^\kappa T^a q' | 0 \rangle \\ &\times \text{Tr} [\Gamma (g_{\mu\nu} \gamma_\lambda + g_{\nu\lambda} \gamma_\mu - 5g_{\mu\lambda} \gamma_\nu - 3i\varepsilon_{\mu\nu\lambda\rho} \gamma^\rho \gamma_5)], \end{aligned} \quad (37)$$



FIG. 8: A diagram for the OPE of the correlation function (8). At the leading accuracy in α_s , this diagram determines the power correction induced by the dimension-6 operators.

which can be derived straightforwardly using the equations of motion, $\not{D}q = 0$, $D^\nu G_{\mu\nu}^a = g \sum_{q'} \bar{q}' \gamma_\mu T^a q'$, where the summation $\sum_{q'}$ is over all quark flavors. Thus, Eq.(36) yields

$$\text{Tr} [\Gamma_1 P_+ \Gamma_2] \frac{ig^2}{1152} (v \cdot x) x^2 \langle 0 | \bar{q} \gamma_\kappa T^a q \sum_{q'} \bar{q}' \gamma^\kappa T^a q' | 0 \rangle, \quad (38)$$

which implies the new power-correction term in the RHS of Eq. (20) with $X = F$, given as [20, 21]

$$+ \frac{\pi C_F \alpha_s}{24 N_c \omega^4} \langle \bar{q} q \rangle^2, \quad (39)$$

where, as usual, the four-quark condensate in Eq.(38) is reduced to the square of $\langle \bar{q} q \rangle$ using the factorization approximation through the vacuum saturation. As the result, the RHS of Eq.(27) receives the new term [20, 21],

$$+ \frac{\pi C_F \alpha_s}{72 N_c M^3} \langle \bar{q} q \rangle^2. \quad (40)$$

Similarly, we can calculate the new corrections to the sum rules (34) and (35) for $\lambda_{E,H}^2$, induced by the dimension-6 operators: at the leading accuracy in α_s , all the relevant power corrections to Eq.(20) with $X = 3H, 3S$ are generated from the second term in Eq.(29). The leading contribution in the ellipses in Eq.(31) is associated with the dimension-6 operators and reads

$$\begin{aligned} & x^\lambda \langle 0 | \bar{q}(0) g G_{\mu\nu}(0) \Gamma_1 P_+ \Gamma_2 D_\lambda q(0) | 0 \rangle \\ &= -\frac{iv \cdot x}{96} g^2 \langle 0 | \bar{q} \gamma_\kappa T^a q \sum_{q'} \bar{q}' \gamma^\kappa T^a q' | 0 \rangle (\text{Tr} [\sigma_{\mu\nu} \Gamma_1 P_+ \Gamma_2] \\ & \quad + 2 \text{Tr} [(iv_\mu \gamma_\nu - iv_\nu \gamma_\mu) \Gamma_1 P_+ \Gamma_2]), \end{aligned} \quad (41)$$

where the matrix element has been handled using Eq.(37) with the indices μ and ν antisymmetrized. Diagrammatically, this result is represented in Fig.8. Eq.(41) implies the new power-correction term in the RHS of Eq. (20), given as

$$+ \frac{\pi C_F \alpha_s}{24 N_c \omega^2} \langle \bar{q} q \rangle^2, \quad + \frac{\pi C_F \alpha_s}{12 N_c \omega^2} \langle \bar{q} q \rangle^2, \quad (42)$$

for $X = 3H, 3S$, respectively, so that we find that Eqs. (34), (35) receive the new terms,

$$+ \frac{\pi C_F \alpha_s}{2 N_c M} \langle \bar{q} q \rangle^2, \quad + \frac{\pi C_F \alpha_s}{N_c M} \langle \bar{q} q \rangle^2, \quad (43)$$

respectively, in their RHS.

We now discuss the effect of the above-obtained power corrections due to the dimension-6 condensates on the corresponding sum rules. First of all, when including Eq.(40) in the sum rule (27), only this new term is of $O(\alpha_s)$, in contrast to the other terms arising in the RHS of Eq.(27), and, actually, the effect of this new term turns out to be completely negligible. This is demonstrated in Fig. 9; here, the dashed curve is almost indistinguishable from the solid curve, and the former is same as the solid curve in Fig. 7.

For the case of the sum rules (34) and (35) for $\lambda_{E,H}^2$, the terms in the RHS, except the term associated with the mixed condensate $\langle \bar{q} g G \cdot \sigma q \rangle$, are of $O(\alpha_s)$ similarly as the new contributions of Eq.(43). The quantitative roles of these new terms are shown in Figs. 10, 11: we calculate Eq.(34) with and without taking into account Eq.(43), and divide both the results by Eq.(27), yielding the solid and dashed curves, respectively, plotted in Fig. 10. The similar calculation based on Eq.(35) yields the solid and dashed curves in Fig. 11; note that the latter curve is same as the dot-dashed curve in Fig. 6 because the dimension-5 condensate does not contribute to Eq.(35). The new contributions of Eq.(43) enhance the values of λ_H^2 and $\lambda_H^2 - \lambda_E^2$, giving rise to some additional dependence on the Borel parameter M , but the effect is not so significant. Indeed, the comparison of Figs. 10 and 11 with Figs. 5 and 6, respectively, indicates that the effects of Eq.(43) due to the dimension-6 condensates are smaller than the dominant effects from the lower-dimensional condensates, such that the convergence of the OPE (20) with $X = 3S$ as well as $X = 3H$ may be suggested at this level of power corrections.

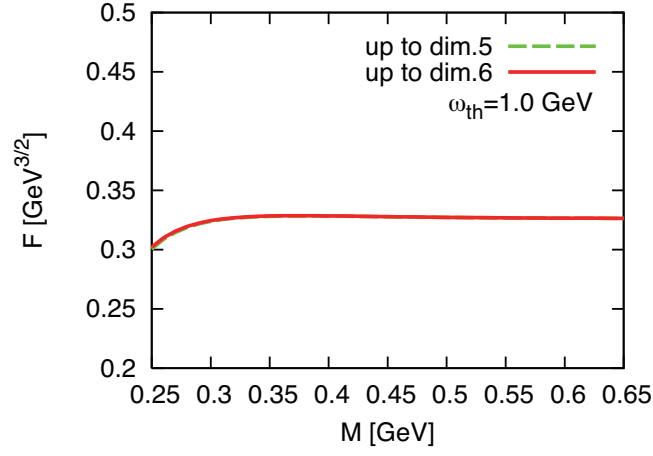


FIG. 9: Borel sum rule for F using $\mu = 1$ GeV, $\omega_{\text{th}} = 1.0$ GeV, and $\bar{\Lambda} = 0.55$ GeV, with and without adding Eq.(40) to the RHS of Eq.(27). Two curves are almost indistinguishable.

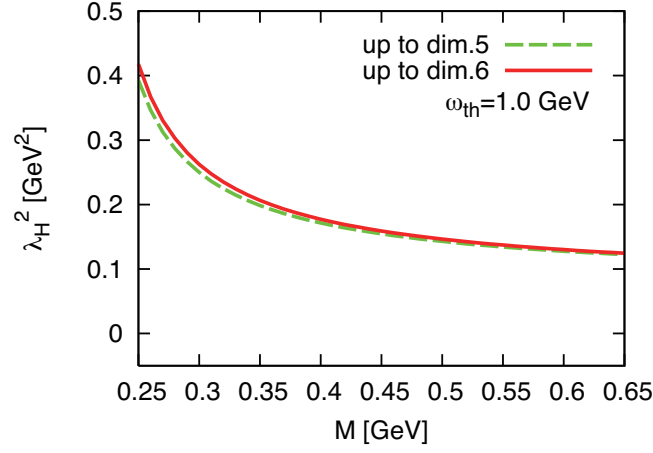


FIG. 10: Borel sum rule for λ_H^2 with $\mu = 1$ GeV and $\omega_{\text{th}} = 1.0$ GeV, calculating Eq.(34) with and without taking into account Eq.(43), and dividing the results by Eq.(27).

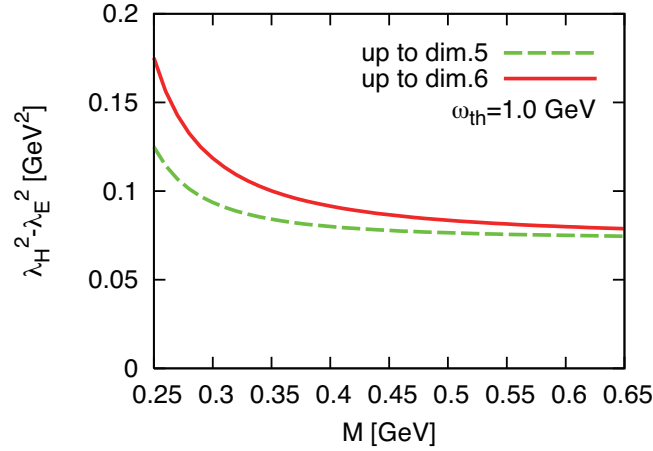


FIG. 11: Same as Fig. 10, but for $\lambda_H^2 - \lambda_E^2$, calculating Eq.(35) with and without taking into account Eq.(43), and dividing the results by Eq.(27).

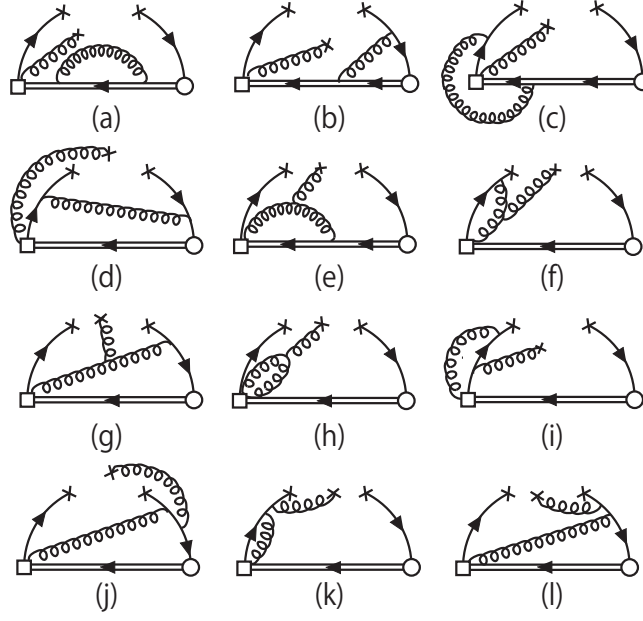


FIG. 12: Feynman diagrams for the one-loop matching of the Wilson coefficients associated with the dimension-5 operators.

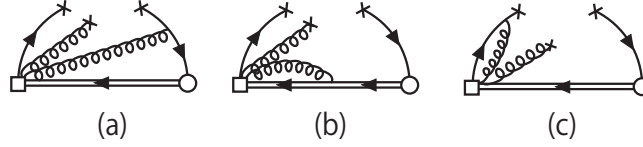


FIG. 13: Examples of the vanishing diagrams for the one-loop corrections to the correlator (8) in the Fock-Schwinger gauge.

IV. ONE-LOOP WILSON COEFFICIENTS FOR THE DIMENSION-5 OPERATORS

The Wilson coefficients arising in the OPE (20) are in general expressed as a power series in α_s ,

$$C_k^X(\omega) = C_k^{X(0)}(\omega) + \frac{\alpha_s}{4\pi} C_k^{X(1)}(\omega) + \dots \quad (44)$$

In particular, for the case with $X = 3H, 3S$, the formulas (32), (33) and (42) indicate $C_k^{X(0)}(\omega) = 0$, for the coefficients associated with the operators of dimension $d \leq 6$, except for $k = \sigma$ and $X = 3H$. Those formulas also give the explicit nonzero results of $C_k^{3H(1)}(\omega)$ and $C_k^{3S(1)}(\omega)$, except for the case with $k = \sigma$, whose results have been unknown. In this section, we derive $C_\sigma^{3H(1)}(\omega)$ and $C_\sigma^{3S(1)}(\omega)$, performing the one-loop matching calculation. The OPE (20) with this result allows us to construct the sum rules for λ_H^2 and $\lambda_H^2 - \lambda_E^2$, taking into account all the relevant $O(\alpha_s)$ effects.

The Feynman diagrams in Fig. 12 represent the one-loop corrections to the correlation function in the LHS of Eq.(8), which are relevant to the matching to derive $C_\sigma^{X(1)}(\omega)$ for $X = 3H, 3S$; here, the corrections due to self-energy insertions into the quark or gluon external fields have been omitted, because the corresponding contributions eventually cancel in the matching. We calculate those Feynman diagrams in $D = 4 + 2\epsilon$ dimensions and derive $C_\sigma^{X(1)}(\omega)$ in the $\overline{\text{MS}}$ scheme. It is convenient to use the Fock-Schwinger gauge for the classical background gluon field, as in Sec. II. Then, the diagrams containing the subdiagram (a) of Fig. 2, as well as the subdiagram (b) or (c), vanish. Also, for the correlator (8), the diagrams in Fig. 13 vanish; in Fig. 13, the vertex arising from the quark-gluon current $\bar{q}(0)\Gamma_1 g G_{\mu\nu}(0)h_v(0)$ vanishes using Eq.(22), and, indeed, the corresponding contribution is absent from the relevant propagator (30).

Here, for later use, we mention the contribution of the tree diagram (d) in Fig. 1 to the correlator in the LHS of Eq.(8), for the case of D dimensions and under the classical background fields $q(x)$, $\bar{q}(x)$ and $G_{\mu\nu}(x)$ for quarks and

gluons; the corresponding contribution reads (see Eq.(21)),

$$\begin{aligned}
& i \int d^D x e^{-i\omega v \cdot x} \theta(-v \cdot x) \delta^{(D)}(x_\perp) \\
& \quad \times \bar{q}(0) g G_{\mu\nu}(0) \Gamma_1 P_+ \Gamma_2 q(0) \\
& = -\frac{1}{2} \text{Tr} [\sigma_{\mu\nu} \Gamma_1 P_+ \Gamma_2] \hat{\Pi}_{3H}^{\text{tree}}(\omega) \\
& \quad - \frac{1}{2} \text{Tr} [(i v_\mu \gamma_\nu - i v_\nu \gamma_\mu) \Gamma_1 P_+ \Gamma_2] \hat{\Pi}_{3S}^{\text{tree}}(\omega),
\end{aligned} \tag{45}$$

where the extraction of the relevant scalar piece from the arising combination of the classical fields is implicit in the LHS, yielding the RHS that is expressed in a similar form as in the RHS of Eq.(8), with

$$\begin{aligned}
\hat{\Pi}_{3H}^{\text{tree}}(\omega) &= \frac{1}{2D(D-1)\omega} \mathcal{O}, \\
\hat{\Pi}_{3S}^{\text{tree}}(\omega) &= 0,
\end{aligned} \tag{46}$$

in terms of the dimension-5 quark-gluon scalar operator,

$$\mathcal{O} = \bar{q} g G \cdot \sigma q. \tag{47}$$

When $D \rightarrow 4$ and $\mathcal{O} \rightarrow \langle \bar{q} g G \cdot \sigma q \rangle$, Eq.(45) reduces to the corresponding contribution using the first term in the RHS of Eq.(31).

Now, it is straightforward to calculate the diagrams in Fig. 12 combining the relevant propagators (21), (23), (30) with other (familiar) building blocks, and it is convenient to perform the loop integrations in the coordinate space: the diagrams (e)-(g) and (i)-(j) in Fig. 12 represent the contributions generated by the second term in the RHS of Eq.(30) and of Eq.(23), respectively, and the diagram (h) can be calculated similarly; on the other hand, from the “nonlocal quark condensate” contributions contained in the ellipses in Eq.(29), the diagrams (k), (l) are generated as the subleading terms in the Taylor expansion similar as in Eq.(25). We note that the diagrams (a)-(c) and (e) all give the UV-divergent results, while the diagrams (g), (j) and (l) give the IR-divergent results. Each of the diagrams (f), (h), (i) and (k) vanishes as a result of the “canceling” UV and IR poles, $1/\epsilon_{UV} - 1/\epsilon_{IR}$, arising from the scaleless loop integral. On the other hand, the diagram (d) yields the result of $\mathcal{O}(\epsilon)$ and vanishes as $D \rightarrow 4$. On the LHS of Eq.(8), in addition to the contributions from all the diagrams in Fig. 12, we have also the counter-term contribution,

$$\begin{aligned}
& \left[-(Z_h - 1) + \left(\frac{\sqrt{Z_2} \sqrt{Z_h}}{Z_J} - 1 \right) \right] \\
& \times \left(-\frac{1}{2} \text{Tr} [\sigma_{\mu\nu} \Gamma_1 P_+ \Gamma_2] \hat{\Pi}_{3H}^{\text{tree}}(\omega) \right) + \dots,
\end{aligned} \tag{48}$$

with $\hat{\Pi}_{3H}^{\text{tree}}(\omega)$ defined as Eqs. (45), (46). Z_h and Z_2 are the quark-field renormalization constants for heavy- and light-quarks, respectively, in the $\overline{\text{MS}}$ scheme using the Feynman gauge for the quantum part of the gluon field, as

$$Z_h = 1 - \frac{C_F \alpha_s}{2\pi\hat{\epsilon}}, \quad Z_2 = 1 + \frac{C_F \alpha_s}{4\pi\hat{\epsilon}}, \tag{49}$$

at one-loop order [2], where $1/\hat{\epsilon} \equiv 1/\epsilon + \gamma_E - \ln 4\pi$, with γ_E the Euler constant, and, similarly, Z_J is the renormalization constant for the heavy-light current operator $J \equiv \bar{h}_v \Gamma_2 q$ in Eq.(8), as

$$J^{\text{ren}} = \frac{1}{Z_J} J^{\text{bare}}, \quad Z_J = 1 - \frac{3C_F \alpha_s}{8\pi\hat{\epsilon}}, \tag{50}$$

connecting the renormalized and bare operators at one-loop order [2]. In Eq.(48), the remaining counter terms, associated with the renormalization of the quark-gluon three-body current operator $\bar{q} \Gamma_1 g G_{\mu\nu} h_v$ in Eq.(8), are represented by the ellipses whose explicit formula is given in Eq.(A3) in Appendix A.

We combine the sum of the contributions of all the diagrams in Fig. 12 with the counter-term contribution (48), and decompose the result as in the RHS of Eq.(8), denoting the corresponding two correlation functions as $\hat{\Pi}_{3H}^{1\text{-loop}}(\omega)$

and $\hat{\Pi}_{3S}^{1\text{-loop}}(\omega)$ in place of $\Pi_{3H,3S}(\omega)$. We obtain, for $\omega < 0$,

$$\begin{aligned} \hat{\Pi}_{3H}^{1\text{-loop}}(\omega) = & \frac{\alpha_s}{96\pi\omega} \left[\frac{2}{N_c\hat{\epsilon}} - \left(N_c - \frac{6}{N_c} \right) \ln \frac{-2\omega}{\mu} \right. \\ & \left. + \frac{5}{2}N_c - \frac{10}{3N_c} + \dots \right] \mathcal{O}, \end{aligned} \quad (51)$$

$$\hat{\Pi}_{3S}^{1\text{-loop}}(\omega) = \frac{\alpha_s}{96\pi\omega} \left[N_c \ln \frac{-2\omega}{\mu} + \frac{1}{2N_c} + \dots \right] \mathcal{O}, \quad (52)$$

with the ellipses denoting the terms that vanish as $\epsilon \rightarrow 0$. Here and below, μ is the $\overline{\text{MS}}$ scale and $\alpha_s \equiv \alpha_s(\mu)$. In the calculation to derive these results, we observe that the UV poles from the diagrams (a) and (b) are canceled, respectively, by the first and second counter-terms in Eq.(48). Similarly, the UV poles from the diagrams (c) and (e), as well as the UV poles from the diagrams (f), (h), (i) and (k) due to the above-mentioned $1/\epsilon_{UV} - 1/\epsilon_{IR}$ structure, are completely canceled by the UV poles arising in the ellipses in Eq.(48), i.e., by the counter terms (A3). Then, the remaining $1/\epsilon$ poles from the diagrams in Fig. 12 are the IR poles only, as it should be, and the sum of all those IR poles yields the $1/\epsilon$ pole in the above results (51), (52).

As a useful cross-check of our results (51), (52), we performed the corresponding NLO calculation also for the correlation function,

$$i \int d^D x e^{i\omega v \cdot x} \langle 0 | T [\bar{q}(x) \Gamma_1 g G_{\mu\nu}(x) h_v(x) \bar{h}_v(0) \Gamma_2 q(0)] | 0 \rangle. \quad (53)$$

Because the Fock-Schwinger gauge, $x^\mu A_\mu(x) = 0$, used in the present paper, violates translational invariance, the calculation of Eq.(53) does not coincide on a diagram-by-diagram basis with that of the LHS in Eq.(8); e.g., for the correlator (53), the contributions of the diagrams (a)-(c) in Fig. 13 do not vanish. With the similar technique as above and with $\epsilon_{IR} = \epsilon_{UV}$, we calculate the contributions to Eq.(53) taking into account all the relevant diagrams, i.e., the diagrams in Figs. 12, 13, and some other nonvanishing diagrams. We find that this calculation yields the results identical to Eqs. (51), (52). Indeed, for example, considering the diagram (e) in Fig. 12 and the diagram (b) in Fig. 13, the sum of the contributions of these diagrams for Eq.(53) coincides with the corresponding sum for Eq.(8). This reflects the fact that the translational invariance is restored in a gauge-invariant subset of the diagrams; note that the contributions of the diagrams involving the subdiagrams in Fig. 2 vanish for Eq.(53), as well as for Eq.(8). Similarly, the diagrams (g), (j), (l) in Fig. 12, the diagram (a) in Fig. 13, and some other diagrams form a gauge-invariant subset, such that they are obtained from the diagram (b) in Fig. 1 by attaching an external gluon line in all possible ways, and we observe that the sum of the contributions of those diagrams is identical between Eq.(53) and Eq.(8). With $\epsilon_{IR} = \epsilon_{UV}$, each of the remaining diagrams in Figs. 12, 13 actually yields the identical result for both Eqs. (53) and (8).

The matching relations of our above results (45)-(46), (51) and (52) with the corresponding term in the OPE (20) read ($X = 3H, 3S$),

$$\hat{\Pi}_X^{\text{tree}}(\omega) + \hat{\Pi}_X^{1\text{-loop}}(\omega) = C_\sigma^X(\omega) \mathcal{O}^{\text{ren}}, \quad (54)$$

for $-\omega \gg \Lambda_{\text{QCD}}$, with the Wilson coefficients expressed as Eq.(44), and the renormalized composite operator \mathcal{O}^{ren} corresponding to Eq.(47), such that $\langle 0 | \mathcal{O}^{\text{ren}} | 0 \rangle = \langle \bar{q} g G \cdot \sigma q \rangle$. Here, the renormalized operator \mathcal{O}^{ren} is related to the bare operator $\mathcal{O}^{\text{bare}}$, and to the operator \mathcal{O} which arises in Eqs. (46), (51) and (52) and is composed of the classical (renormalized) constituent fields, as

$$\mathcal{O}^{\text{ren}} = \frac{1}{Z_\mathcal{O}} \mathcal{O}^{\text{bare}} = \frac{Z_2}{Z_\mathcal{O}} \mathcal{O}, \quad (55)$$

with Z_2 of Eq.(49), noting that the combination $g G_{\mu\nu}$ is not renormalized in the background field method [24]. To obtain $Z_\mathcal{O}$, we performed the one-loop renormalization of the dimension-5 quark-gluon-mixed operator (47) in the present framework with the $\overline{\text{MS}}$ scheme, and the result is (see the discussion below Eq.(A5) in Appendix A)

$$Z_\mathcal{O} = 1 + \frac{\alpha_s}{8\pi\hat{\epsilon}} \left(N_c - \frac{5}{N_c} \right), \quad (56)$$

which coincides with the corresponding result calculated in Ref. [25]. Now, the matching of the $O(\alpha_s^0)$ terms of both sides in Eq.(54) immediately yields

$$\begin{aligned} C_\sigma^{3H(0)}(\omega) &= \frac{1}{4(2+\epsilon)(3+2\epsilon)\omega}, \\ C_\sigma^{3S(0)}(\omega) &= 0, \end{aligned} \quad (57)$$

for arbitrary ϵ , and these results reproduce the corresponding formulas in Eqs. (32) and (33) as $\epsilon \rightarrow 0$. The one-loop matching due to the $O(\alpha_s)$ terms in Eq.(54) leads to the relation,

$$\frac{\alpha_s}{4\pi} C_\sigma^{3X(1)}(\omega) = \frac{\partial \hat{\Pi}_{3X}^{1\text{-loop}}(\omega)}{\partial \mathcal{O}} - \left(\frac{Z_2}{Z_\mathcal{O}} - 1 \right) C_\sigma^{3X(0)}(\omega), \quad (58)$$

the both sides of which are finite as $\epsilon \rightarrow 0$: for $X = 3H$, the second term in the RHS serves to cancel the $1/\epsilon$ pole arising in the first term (see Eq.(51)), while, for $X = 3S$, Eq.(57) implies that $C_\sigma^{3S(1)}(\omega)$ is directly given by the coefficient of \mathcal{O} in Eq.(52). Substituting the $\epsilon \rightarrow 0$ limit of Eqs. (57) and (58) into Eq.(44), we obtain the final form of the corresponding NLO Wilson coefficients,

$$C_\sigma^{3H}(\omega) = \frac{1}{24\omega} \left[1 - \frac{\alpha_s}{4\pi} \left\{ \left(N_c - \frac{6}{N_c} \right) \ln \frac{-2\omega}{\mu} - \frac{5}{2} N_c + \frac{1}{N_c} \right\} \right], \quad (59)$$

$$C_\sigma^{3S}(\omega) = \frac{\alpha_s}{96\pi\omega} \left[N_c \ln \frac{-2\omega}{\mu} + \frac{1}{2N_c} \right], \quad (60)$$

in the $\overline{\text{MS}}$ scheme.

V. RENORMALIZATION-GROUP IMPROVEMENT AND BOREL ANALYSIS

We substitute the new results (59) and (60) into the Wilson coefficient $C_\sigma^X(\omega)$ of Eq.(20), while, for the other coefficients $C_I^X(\omega)$, $C_q^X(\omega)$, and $C_G^X(\omega)$, we have the corresponding formulas in Eqs. (32) and (33); furthermore, we add the new power-correction term with (42) to the RHS of Eq.(20). The result gives our upgraded OPEs for the correlation functions in Eq.(8), taking into account the operators of dimension $d \leq 6$ and the associated Wilson coefficients to the $O(\alpha_s)$ accuracy. Now, we use these new results for the OPE to derive the sum rules for λ_H^2 and $\lambda_H^2 - \lambda_E^2$: we substitute these OPEs into Eqs. (18) and (19); here, it is straightforward to calculate the discontinuities of the coefficients (59) and (60) across the cut along the line $\omega > 0$ in the complex ω plane, reexpressing the logarithmic contributions as $(2/\omega) \ln(-2\omega/\mu) = (d/d\omega) \ln^2(-2\omega/\mu)$. As a result, we obtain the new formulas of the Borel sum rules for λ_H^2 and $\lambda_H^2 - \lambda_E^2$,

$$\begin{aligned} F^2(\mu) \lambda_H^2(\mu) e^{-\bar{\Lambda}/M} &= -\frac{2\alpha_s}{\pi^3} N_c C_F M^5 W^{(4)}\left(\frac{\omega_{\text{th}}}{M}\right) \\ &\quad - \frac{3\alpha_s}{\pi} C_F M^2 \langle \bar{q}q \rangle W^{(1)}\left(\frac{\omega_{\text{th}}}{M}\right) \\ &\quad + \frac{M}{4} \left\langle \frac{\alpha_s}{\pi} G^2 \right\rangle W^{(0)}\left(\frac{\omega_{\text{th}}}{M}\right) \\ &\quad - \frac{1}{4} \langle \bar{q}gG \cdot \sigma q \rangle \left[1 - \frac{\alpha_s}{4\pi} \left\{ -\frac{5}{2} N_c + \frac{1}{N_c} \right. \right. \\ &\quad \left. \left. + \left(N_c - \frac{6}{N_c} \right) \left(\ln \frac{2M}{\mu e^{\gamma_E}} - \Gamma(0, \frac{\omega_{\text{th}}}{M}) \right) \right\} \right] \\ &\quad + \frac{\pi C_F \alpha_s}{2N_c M} \langle \bar{q}q \rangle^2, \end{aligned} \quad (61)$$

and

$$\begin{aligned} F^2(\mu) [\lambda_H^2(\mu) - \lambda_E^2(\mu)] e^{-\bar{\Lambda}/M} &= \frac{2\alpha_s}{\pi^3} N_c C_F M^5 W^{(4)}\left(\frac{\omega_{\text{th}}}{M}\right) \\ &\quad - \frac{3\alpha_s}{\pi} C_F M^2 \langle \bar{q}q \rangle W^{(1)}\left(\frac{\omega_{\text{th}}}{M}\right) \\ &\quad + \frac{M}{4} \left\langle \frac{\alpha_s}{\pi} G^2 \right\rangle W^{(0)}\left(\frac{\omega_{\text{th}}}{M}\right) \\ &\quad - \langle \bar{q}gG \cdot \sigma q \rangle \frac{\alpha_s}{16\pi} \left[N_c \left(\ln \frac{2M}{\mu e^{\gamma_E}} - \Gamma(0, \frac{\omega_{\text{th}}}{M}) \right) + \frac{1}{2N_c} \right] \\ &\quad + \frac{\pi C_F \alpha_s}{N_c M} \langle \bar{q}q \rangle^2, \end{aligned} \quad (62)$$

where $W^{(m)}(\omega_{\text{th}}/M)$ is defined as Eq.(28) and

$$\Gamma(a, z) = \int_z^\infty dt t^{a-1} e^{-t} \quad (63)$$

is the incomplete Gamma function. These two sum rules, (61) and (62), are the new results that take into account the operators of dimension $d \leq 6$ and the associated Wilson coefficients to the $O(\alpha_s)$ accuracy: compared with the previous results (34) and (35) that correspond to Grozin-Neubert's sum rule formulas [9], Eqs. (61) and (62) receive the $O(\alpha_s)$ corrections associated with the dimension-5 quark-gluon-mixed condensate $\langle \bar{q}gG \cdot \sigma q \rangle$, as well as Eq.(43) due to the dimension-6 four-quark condensate $\langle \bar{q}q \rangle^2$. In particular, the former corrections bring an explicit dependence on the scale μ to the RHS of Eqs. (61) and (62), through the logarithmic term, $\ln(2M/\mu e^{\gamma_E})$: one can show that $\lambda_{E,H}^2(\mu)$ determined by our formulas (61) and (62) satisfy the renormalization-group equations of Eqs. (A4), (A5), taking into account the derivative of the above logarithm $\ln(2M/\mu e^{\gamma_E})$, as well as the scale dependence of the other terms controlled by the nontrivial anomalous dimensions:

$$\left(\mu \frac{d}{d\mu} + \gamma_J(\alpha_s) \right) F(\mu) = 0, \quad (64)$$

$$\left(\mu \frac{d}{d\mu} + \gamma_q(\alpha_s) \right) \langle \bar{q}q \rangle(\mu) = 0, \quad (65)$$

$$\left(\mu \frac{d}{d\mu} + \gamma_\sigma(\alpha_s) \right) \langle \bar{q}gG \cdot \sigma q \rangle(\mu) = 0, \quad (66)$$

$$\gamma_k(\alpha_s) = \gamma_{k0} \frac{\alpha_s}{4\pi} + \gamma_{k1} \left(\frac{\alpha_s}{4\pi} \right)^2 + \dots \quad (k = J, q, \sigma), \quad (67)$$

where

$$\gamma_{J0} = -3C_F, \quad \gamma_{q0} = -6C_F, \quad \gamma_{\sigma0} = N_c - \frac{5}{N_c}, \quad (68)$$

$$\begin{aligned} \gamma_{J1} = C_F \left[\left(\frac{5}{2} - \frac{8}{3}\pi^2 \right) C_F \right. \\ \left. + \left(\frac{2}{3}\pi^2 - \frac{49}{6} \right) N_c + \frac{5}{3}N_f \right], \end{aligned} \quad (69)$$

$$\gamma_{q1} = -C_F \left(3C_F + \frac{97}{3}N_c - \frac{10}{3}N_f \right), \quad (70)$$

while $\gamma_{\sigma1}$ is not available. For the present purpose to confirm Eq.(A4) with the one-loop mixing matrix (A5), the explicit forms of γ_{J0} and $\gamma_{\sigma0}$ in Eq.(68), combined with $d\Lambda/d\mu = 0$ [2], are sufficient, where the former are immediate consequences of the corresponding renormalization constants (50), (56) [38]. Apparently, Grozin-Neubert's sum-rule formulas given by Eqs. (34) and (35) do not obey such renormalization-group property. Thus, our sum rules (61) and (62) allow the first nonperturbative estimate of the HQET parameters $\lambda_{E,H}^2(\mu)$ with the correct μ -dependence implemented. We emphasize that the new $O(\alpha_s)$ corrections in Eqs. (61) and (62), associated with the dimension-5 quark-gluon-mixed condensate $\langle \bar{q}gG \cdot \sigma q \rangle$, play essential roles to reproduce renormalization-group equations of Eqs. (A4), (A5) in the QCD sum-rule framework.

It is worth comparing this remarkable property of Eqs. (61) and (62) with the situation for the case of the sum rules of the decay constant $F(\mu)$, based on the correlator (7): $F(\mu)$ determined from the sum rule (27), which was presented in Sec. II at the leading accuracy in α_s , does not obey Eq.(64), even though we take into account the scale dependence of Eqs. (65), (66) in Eq.(27). Now, including the higher-order contributions, the $O(\alpha_s)$ corrections for the relevant Wilson coefficients and the dimension-6 condensate contribution (40), Eq.(27) is modified into [10, 21, 28]

$$\begin{aligned} F^2(\mu) e^{-\bar{\Lambda}/M} = \frac{N_c M^3}{\pi^2} \int_0^{\omega_{\text{th}}/M} dz z^2 e^{-z} \\ \times \left[1 + \frac{3C_F \alpha_s}{2\pi} \left(\ln \frac{\mu}{2Mz} + \frac{17}{6} + \frac{2\pi^2}{9} \right) \right] \\ - \langle \bar{q}q \rangle \left[1 + \frac{3C_F \alpha_s}{2\pi} \right] \\ + \frac{1}{16M^2} \langle \bar{q}gG \cdot \sigma q \rangle \end{aligned}$$

$$+ \frac{\pi C_F \alpha_s}{72 N_c M^3} \langle \bar{q}q \rangle^2. \quad (71)$$

Here, in particular, the $O(\alpha_s)$ corrections arising in the second line bring an explicit dependence on the scale μ , through the logarithm $\ln(\mu/2Mz)$. Taking into account this new μ -dependence, $F(\mu)$ determined by Eq.(71) obeys the renormalization-group equation (64), up to the corrections of $O(\alpha_s^2)$ and the small contributions from the condensates of dimension-5 and higher (see Figs. 7, 9).

The correct renormalization-group properties obeyed by Eqs. (61), (62) and (71) allow us to improve these sum rules further, such that the logarithmic effects associated with $\alpha_s \ln(M/\mu)$ are resummed to all orders. This renormalization-group improvement is formally achieved by setting $\mu = \mu'$ ($\mu' \sim M$) in Eqs. (61), (62) and (71), followed by evolving the resulting HQET parameters and the condensates at the scale μ' to those at $\mu \sim 1$ GeV: using the first two coefficients of the β function,

$$\begin{aligned} \beta_0 &= \frac{11}{3} N_c - \frac{2}{3} N_f, \\ \beta_1 &= \frac{34}{3} N_c^2 - \frac{10}{3} N_c N_f - 2 C_F N_f, \end{aligned} \quad (72)$$

with N_f being the number of active flavors, the corresponding renormalization-group-improved sum rule for the decay constant reads

$$\begin{aligned} &F^2(\mu') e^{-\bar{\Lambda}/M} \\ &= \frac{N_c M^3}{\pi^2} \int_0^{\omega_{\text{th}}/M} dz z^2 e^{-z} \\ &\quad \times \left[1 + \frac{3 C_F \alpha_s(\mu')}{2\pi} \left(\ln \frac{\mu'}{2Mz} + \frac{17}{6} + \frac{2\pi^2}{9} \right) \right] \\ &\quad - \left(\frac{\alpha_s(\mu')}{\alpha_s(\mu)} \right)^{\frac{\gamma_{q0}}{2\beta_0}} \left[1 + \frac{\alpha_s(\mu') - \alpha_s(\mu)}{4\pi} \frac{\gamma_{q0}}{2\beta_0} \left(\frac{\gamma_{q1}}{\gamma_{q0}} - \frac{\beta_1}{\beta_0} \right) \right] \\ &\quad \times \langle \bar{q}q \rangle(\mu) \left[1 + \frac{3 C_F \alpha_s(\mu')}{2\pi} \right] \\ &\quad + \frac{1}{16M^2} \left(\frac{\alpha_s(\mu')}{\alpha_s(\mu)} \right)^{\frac{\gamma_{q0}}{2\beta_0}} \langle \bar{q}gG \cdot \sigma q \rangle(\mu) \\ &\quad + \frac{\pi C_F \alpha_s(\mu)}{72 N_c M^3} \langle \bar{q}q \rangle^2(\mu), \end{aligned} \quad (73)$$

to be combined with

$$\begin{aligned} F^2(\mu) &= F^2(\mu') \left(\frac{\alpha_s(\mu)}{\alpha_s(\mu')} \right)^{\frac{\gamma_{J0}}{\beta_0}} \left[1 + \frac{\alpha_s(\mu) - \alpha_s(\mu')}{4\pi} \right. \\ &\quad \left. \times \frac{\gamma_{J0}}{\beta_0} \left(\frac{\gamma_{J1}}{\gamma_{J0}} - \frac{\beta_1}{\beta_0} \right) \right]. \end{aligned} \quad (74)$$

Here, we have neglected the unknown NLO-level effects associated with the dimension-5 quark-gluon-mixed condensate, i.e., the corresponding one-loop coefficient function and two-loop anomalous dimension, and also neglected the running of the dimension-6 four-quark condensate. Up to these small effects, Eq.(73) combined with Eq.(74) sums up the leading and next-to-leading logarithms of the form $\alpha_s^n \ln^n(M/\mu)$ and $\alpha_s^{n+1} \ln^n(M/\mu)$.

As a result of the similar renormalization-group improvement for the two sum rules (61) and (62), we obtain

$$\begin{aligned}
F^2(\mu') \lambda_H^2(\mu') e^{-\bar{\Lambda}/M} = & -\frac{2\alpha_s(\mu')}{\pi^3} N_c C_F M^5 W^{(4)}\left(\frac{\omega_{\text{th}}}{M}\right) \\
& -\frac{3\alpha_s(\mu')}{\pi} C_F M^2 \left(\frac{\alpha_s(\mu')}{\alpha_s(\mu)}\right)^{\frac{\gamma_{q0}}{2\beta_0}} \langle \bar{q}q \rangle(\mu) \\
& \times W^{(1)}\left(\frac{\omega_{\text{th}}}{M}\right) + \frac{M}{4} \langle \frac{\alpha_s}{\pi} G^2 \rangle W^{(0)}\left(\frac{\omega_{\text{th}}}{M}\right) \\
& -\frac{1}{4} \left(\frac{\alpha_s(\mu')}{\alpha_s(\mu)}\right)^{\frac{\gamma_{q0}}{2\beta_0}} \langle \bar{q}gG \cdot \sigma q \rangle(\mu) \\
& \times \left[1 - \frac{\alpha_s(\mu')}{4\pi} \left\{ -\frac{5}{2} N_c + \frac{1}{N_c} \right. \right. \\
& \left. \left. + \left(N_c - \frac{6}{N_c} \right) \left(\ln \frac{2M}{\mu' e^{\gamma_E}} - \Gamma(0, \frac{\omega_{\text{th}}}{M}) \right) \right\} \right] \\
& + \frac{\pi C_F \alpha_s(\mu)}{2N_c M} \langle \bar{q}q \rangle^2(\mu), \tag{75}
\end{aligned}$$

$$\begin{aligned}
F^2(\mu') [\lambda_H^2(\mu') - \lambda_E^2(\mu')] e^{-\bar{\Lambda}/M} = & \frac{2\alpha_s(\mu')}{\pi^3} N_c C_F M^5 W^{(4)}\left(\frac{\omega_{\text{th}}}{M}\right) \\
& -\frac{3\alpha_s(\mu')}{\pi} C_F M^2 \left(\frac{\alpha_s(\mu')}{\alpha_s(\mu)}\right)^{\frac{\gamma_{q0}}{2\beta_0}} \langle \bar{q}q \rangle(\mu) \\
& \times W^{(1)}\left(\frac{\omega_{\text{th}}}{M}\right) + \frac{M}{4} \langle \frac{\alpha_s}{\pi} G^2 \rangle W^{(0)}\left(\frac{\omega_{\text{th}}}{M}\right) \\
& -\left(\frac{\alpha_s(\mu')}{\alpha_s(\mu)}\right)^{\frac{\gamma_{q0}}{2\beta_0}} \langle \bar{q}gG \cdot \sigma q \rangle(\mu) \\
& \times \frac{\alpha_s(\mu')}{16\pi} \left[N_c \left(\ln \frac{2M}{\mu' e^{\gamma_E}} - \Gamma(0, \frac{\omega_{\text{th}}}{M}) \right) + \frac{1}{2N_c} \right] \\
& + \frac{\pi C_F \alpha_s(\mu)}{N_c M} \langle \bar{q}q \rangle^2(\mu), \tag{76}
\end{aligned}$$

which are to be combined with

$$\left(\frac{\lambda_E^2(\mu)}{\lambda_H^2(\mu)} \right) = \left(\frac{\alpha_s(\mu)}{\alpha_s(\mu')} \right)^{\frac{\gamma_0}{2\beta_0}} \left(\frac{\lambda_E^2(\mu')}{\lambda_H^2(\mu')} \right). \tag{77}$$

Here, the anomalous dimensions for $\lambda_{E,H}^2(\mu)$ are known only at one-loop as Eq.(A5). We can divide Eqs. (75) and (76) by Eq.(73) so as to eliminate the factors $F^2(\mu') e^{-\bar{\Lambda}/M}$, before combining with the evolution (77).

We evaluate the renormalization-group-improved Borel sum rules Eqs. (73), (75) and (76) with $\mu' = 2M$ and $\mu = 1$ GeV; here, the choice $\mu' = 2M$ allows us to sum up the relevant logarithmic contributions. In addition to this default choice, we also study the scale dependence of the results when varying μ' in a range with $\mu' \sim M$; this gives us a rough estimate of the uncertainty of the results due to the neglected part of order α_s^2 , and to the contributions of higher order. We use the input values for the vacuum condensates as given in Table I in Sec. II, and use the two-loop expression for the running coupling $\alpha_s(\mu)$ with $\Lambda_{\text{QCD}}^{(4)} = 0.31$ GeV, so that $\alpha_s(1 \text{ GeV}) \simeq 0.47$, and $\alpha_s(m_B) \simeq 0.21$.

First of all, we note that

$$\begin{aligned}
\hat{F} \equiv F(\mu') \alpha_s(\mu')^{-\frac{\gamma_{J0}}{2\beta_0}} \left(1 - \frac{\alpha_s(\mu')}{8\pi} \delta \right), \tag{78} \\
\delta = \frac{\gamma_{J0}}{\beta_0} \left(\frac{\gamma_{J1}}{\gamma_{J0}} - \frac{\beta_1}{\beta_0} \right),
\end{aligned}$$

corresponding to the μ' -dependent factors in Eq.(74), forms the renormalization-group-invariant combination, for which the Borel analysis has been performed in the literature [10, 11, 21]: substituting Eq.(73) into the RHS of

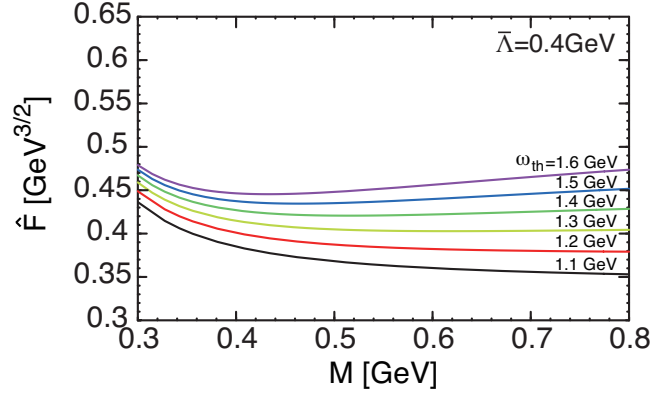


FIG. 14: Borel sum rule for \hat{F} based on Eq.(79) with $\mu' = 2M$ and $\bar{\Lambda} = 0.4$ GeV. From bottom to top, the curves correspond to $\omega_{\text{th}} = 1.1, 1.2, 1.3, 1.4, 1.5, 1.6$ GeV.

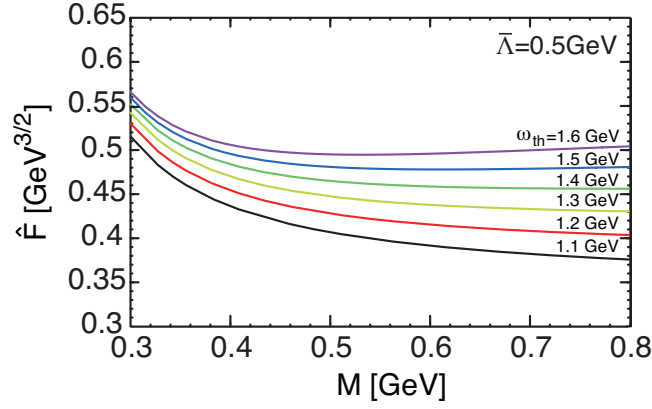


FIG. 15: Borel sum rule for \hat{F} based on Eq.(79) with $\mu' = 2M$ and $\bar{\Lambda} = 0.5$ GeV. From bottom to top, the curves correspond to $\omega_{\text{th}} = 1.1, 1.2, 1.3, 1.4, 1.5, 1.6$ GeV.

Eq.(78), we obtain the sum rule formula for the renormalization-group-invariant decay constant,

$$\begin{aligned}
 & \hat{F}^2 e^{-\bar{\Lambda}/M} \\
 &= \alpha_s(\mu')^{-\frac{\gamma_{M0}}{\beta_0}} \left\{ \frac{N_c M^3}{\pi^2} \int_0^{\omega_{\text{th}}/M} dz z^2 e^{-z} \right. \\
 & \quad \times \left[1 + \frac{3C_F \alpha_s(\mu')}{2\pi} \left(\ln \frac{\mu'}{2Mz} + \frac{17}{6} + \frac{2\pi^2}{9} \right) - \frac{\alpha_s(\mu')}{4\pi} \delta \right] \\
 & \quad - \left(\frac{\alpha_s(\mu')}{\alpha_s(\mu)} \right)^{\frac{\gamma_{q0}}{2\beta_0}} \left[1 + \frac{\alpha_s(\mu') - \alpha_s(\mu)}{4\pi} \frac{\gamma_{q0}}{2\beta_0} \left(\frac{\gamma_{q1}}{\gamma_{q0}} - \frac{\beta_1}{\beta_0} \right) \right. \\
 & \quad \quad \left. + \frac{3C_F \alpha_s(\mu')}{2\pi} - \frac{\alpha_s(\mu')}{4\pi} \delta \right] \langle \bar{q}q \rangle(\mu) \\
 & \quad + \frac{1}{16M^2} \left(\frac{\alpha_s(\mu')}{\alpha_s(\mu)} \right)^{\frac{\gamma_{g0}}{2\beta_0}} \langle \bar{q}gG \cdot \sigma q \rangle(\mu) \\
 & \quad \left. + \frac{\pi C_F \alpha_s(\mu)}{72N_c M^3} \langle \bar{q}q \rangle^2(\mu) \right\}, \tag{79}
 \end{aligned}$$

where $\mu' = 2M$ as the default scale.

In Figs. 14 and 15, we show \hat{F} as a function of M using Eq.(79) with $\bar{\Lambda} = 0.4$ and 0.5 GeV, respectively, corresponding

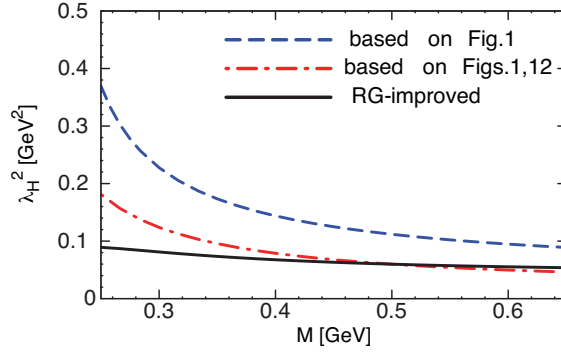


FIG. 16: Borel sum rules for $\lambda_H^2(1 \text{ GeV})$ with the continuum threshold $\omega_{\text{th}} = 1.3 \text{ GeV}$. The dashed curve is based on Fig. 1, the dot-dashed curve is based on Figs. 1 and 12, and the solid curve corresponds to the renormalization-group improvement based on Figs. 1 and 12.

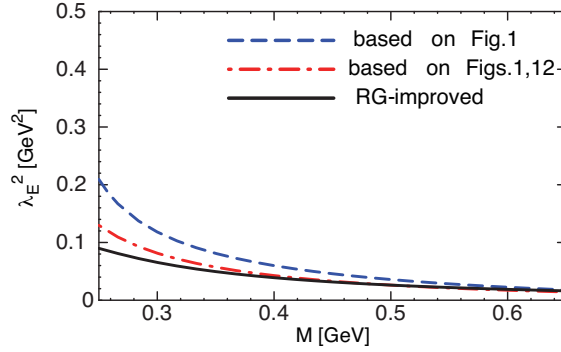


FIG. 17: Same as Fig. 16, but for $\lambda_E^2(1 \text{ GeV})$.

to the choice $\bar{\Lambda} = 0.4\text{--}0.5 \text{ GeV}$ [15, 30], and the curves are drawn for different values of ω_{th} . The stable behaviors are obtained for $M \gtrsim 0.4 \text{ GeV}$ with $1.2 \text{ GeV} \lesssim \omega_{\text{th}} \lesssim 1.4 \text{ GeV}$, yielding $\hat{F} \sim 0.4 \text{ GeV}^{3/2}$. It is worth noting that, by taking into account the corrections due to the finite quark mass m_b , the value of \hat{F} around $0.4 \text{ GeV}^{3/2}$ was shown to be modified into $f_B \simeq 0.2 \text{ GeV}$ [2, 10, 11], which appears to be consistent with the recent lattice results, Eq.(3). It should be noted that Eq.(79) with $\bar{\Lambda} \gtrsim 0.5 \text{ GeV}$ yields the larger \hat{F} as the stable value associated with $\omega_{\text{th}} \gtrsim 1.4 \text{ GeV}$; this would not be favored in view of Eq.(3). Thus, we conclude that the range $\omega_{\text{th}} = 1.2\text{--}1.4 \text{ GeV}$ corresponds to the optimal choice for the threshold parameter [39].

With this choice of the continuum threshold, $\omega_{\text{th}} = 1.2\text{--}1.4 \text{ GeV}$, we will evaluate Borel sum rules for $\lambda_{E,H}^2$. For this purpose, we need not specify the explicit value of $\bar{\Lambda}$, because Eqs. (75) and (76) divided by Eq.(73) do not depend explicitly on $\bar{\Lambda}$. By inspection of the contributions from each term in Eq.(73), we find that, for $M \gtrsim 0.4 \text{ GeV}$, the contribution of the perturbative correction terms is less than $\sim 40\%$ in the OPE for the sum rule and the contribution of the nonperturbative power correction terms is much smaller. On the other hand, for $M \lesssim 0.6 \text{ GeV}$, the contribution of the higher resonances and continuum contributions is less than $\sim 40\%$ of the total contribution in the dispersion relation for the sum rule. Thus, we take $0.4 \text{ GeV} \lesssim M \lesssim 0.6 \text{ GeV}$ as the stability window in the following calculations of Eqs. (75) and (76). The correction terms, as well as the higher resonances and continuum contributions, arising in the sum rules (75), (76), are under control for this window.

In Figs. 16 and 17 we show the results for $\lambda_H^2(\mu = 1 \text{ GeV})$ and $\lambda_E^2(\mu = 1 \text{ GeV})$, respectively, as functions of the Borel parameter M , using the continuum threshold $\omega_{\text{th}} = 1.3 \text{ GeV}$. The solid curves are obtained by dividing Eqs. (75) and (76) by Eq.(73), followed by the evolution of the results from $\mu' = 2M$ to $\mu = 1 \text{ GeV}$ using Eq.(77), and thus show our full results with the renormalization-group improvement. For comparison, the dot-dashed curves show the “fixed-order” results that are obtained by dividing Eqs. (61) and (62) by Eq.(71), while the dashed curves are obtained by dividing Eqs. (34) and (35) by Eq.(27). The dashed curve in Fig. 16 shows the behavior similar as the curves in Fig. 3, because the difference between those curves are only due to the value of the threshold ω_{th} . The new $O(\alpha_s)$ contributions due to Fig. 12, and also the associated renormalization-group-improvement effects, significantly improve the stability of the sum rules. Furthermore, those contributions significantly reduce the magnitude of λ_H^2 as well as λ_E^2 . For those results, we find that the behavior of the decay constant F , arising in Eqs. (75) and (76), actually

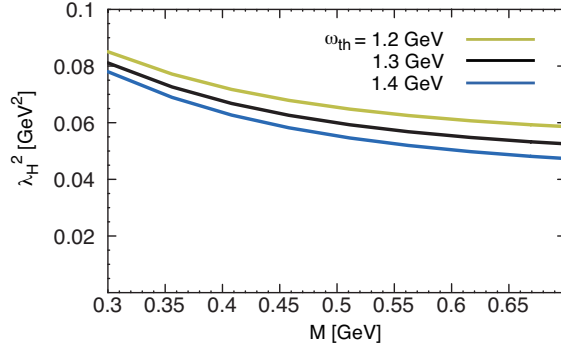


FIG. 18: Borel sum rules for $\lambda_H^2(1 \text{ GeV})$ as the renormalization group improvement based on Figs. 1 and 12. From top to bottom, the curves correspond to $\omega_{\text{th}} = 1.2, 1.3, 1.4 \text{ GeV}$.

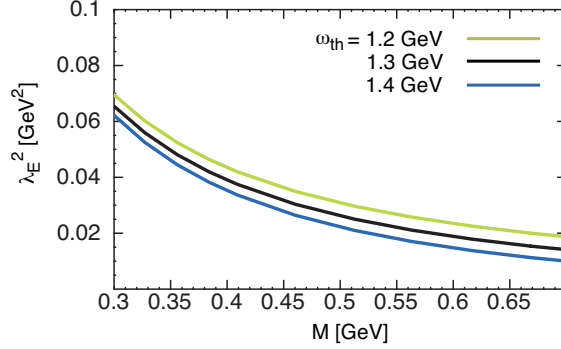


FIG. 19: Same as Fig. 18, but for $\lambda_E^2(1 \text{ GeV})$.

plays important roles: comparing Fig. 9 with Figs. 14, 15, we see the large effects due to the renormalization-group-improved, NLO perturbative corrections in the decay constant sum rule. It is worth mentioning that the corresponding large radiative corrections to the decay constant is mainly due to one-gluon exchange between heavy and light quarks in Feynman gauge, i.e., from their Coulomb interaction, and that those large effects are essential to yield the values consistent with Eq.(3) [2, 10]; on the other hand, it has been demonstrated that the decay constant sum rule (73) is quite stable with respect to inclusion of the NNLO-level radiative corrections [11].

Figs. 18 and 19 show the ω_{th} dependence of the Borel sum rules for $\lambda_H^2(1 \text{ GeV})$ and $\lambda_E^2(1 \text{ GeV})$, respectively, as functions of M , which are obtained by dividing Eqs. (75) and (76) by Eq.(73), followed by the evolution of the results from $\mu' = 2M$ to $\mu = 1 \text{ GeV}$ using Eq.(77); the middle curves in Figs. 18 and 19 are same as the solid curves in Figs. 16 and 17, respectively. We see that the central values are $\lambda_H^2(1 \text{ GeV}) = 0.06 \text{ GeV}^2$ and $\lambda_E^2(1 \text{ GeV}) = 0.03 \text{ GeV}^2$ as an average over the stability window $M = 0.4\text{--}0.6 \text{ GeV}$ and the range $\omega_{\text{th}} = 1.2\text{--}1.4 \text{ GeV}$ for our optimized threshold parameter, and that these central values are associated with the uncertainties $\pm 0.01 \text{ GeV}^2$ and $\pm 0.015 \text{ GeV}^2$, respectively.

To estimate the uncertainties due to the lack of information of two-loop anomalous dimensions as well as the higher-loop effects in Eqs. (75)-(77), the scale dependence of our full results with the renormalization-group improvement is analyzed by varying μ' around the default value $2M$, e.g., for a range $M \lesssim \mu' \lesssim 4M$; if $\mu' = M$ were chosen, $\alpha_s(M)$ would arise in the corresponding formulas with too small scale for perturbation theory in $0.4 \text{ GeV} \lesssim M \lesssim 0.6 \text{ GeV}$. Thus, we vary μ' in the range $1.5M \leq \mu' \leq 4M$, for Eqs. (75) and (76) divided by Eq.(73), followed by the evolution using Eq.(77) from μ' to $\mu = 1 \text{ GeV}$: the corresponding results of $\lambda_{E,H}^2(1 \text{ GeV})$ increase (decrease) for increasing (decreasing) μ' , and we find that the above-mentioned central values, $\lambda_H^2(1 \text{ GeV}) = 0.06 \text{ GeV}^2$ and $\lambda_E^2(1 \text{ GeV}) = 0.03 \text{ GeV}^2$, receive the $\pm 0.02 \text{ GeV}^2$ and $\pm 0.005 \text{ GeV}^2$ variations, respectively.

Similarly, we calculate the uncertainties of the results due to the uncertainties in the input parameters of Table I. We also vary $\Lambda_{\text{QCD}}^{(4)}$ in a range $0.29 \text{ GeV} \lesssim \Lambda_{\text{QCD}}^{(4)} \lesssim 0.33 \text{ GeV}$ corresponding to $\alpha_s(1 \text{ GeV}) = 0.44\text{--}0.5$. Among them, the uncertainty of the dimension-5 quark-gluon-mixed condensate $\langle \bar{q}gG \cdot \sigma q \rangle$ produces the largest effect as $\sim 15\%$ and $\sim 30\%$ of the total contribution to $\lambda_H^2(1 \text{ GeV})$ and $\lambda_E^2(1 \text{ GeV})$, respectively, while each of the other uncertainties yields 10% or less of the total contribution to $\lambda_{E,H}^2(1 \text{ GeV})$.

Adding the errors induced by all source of uncertainties, ω_{th} , μ' , condensates in Table I, and $\Lambda_{\text{QCD}}^{(4)}$, discussed so far in quadrature, we obtain $\pm 0.025 \text{ GeV}^2$ and $\pm 0.018 \text{ GeV}^2$ for $\lambda_H^2(1 \text{ GeV})$ and $\lambda_E^2(1 \text{ GeV})$, respectively. There also exists an overall intrinsic uncertainty of the QCD sum rule method itself which is difficult to estimate. Thus, with a conservative estimate of the uncertainties, our final results read

$$\begin{aligned}\lambda_E^2(1 \text{ GeV}) &= 0.03 \pm 0.02 \text{ GeV}^2, \\ \lambda_H^2(1 \text{ GeV}) &= 0.06 \pm 0.03 \text{ GeV}^2.\end{aligned}\tag{80}$$

Note that the errors in the previous estimate (6) [9] are due only to the choice of the continuum threshold and the dependence on the Borel parameter in the corresponding sum rules using Eqs. (34) and (35).

It would be interesting to compare our estimate (80) with the values of the corresponding quantities of light pseudoscalar mesons, π , K . A straightforward comparison discussed in Appendix B suggests that the values of the quark-antiquark-gluon three-body components have important difference between the B meson and the light π, K mesons, but their orders of magnitude are not largely different. This difference in the values of the three-body components reflects the different behaviors of the corresponding sum rules, where the dimension-5 quark-gluon mixed condensates play dominant role in the heavy-quark limit while those play minor role near the chiral limit.

VI. CONCLUSIONS

We have discussed the QCD sum rule calculation of the HQET parameters λ_E^2 and λ_H^2 , which represent quark-gluon three-body components in the B -meson wavefunction. We have updated the sum rules for $\lambda_{E,H}^2$ calculating the new higher-order contributions to the OPE for the corresponding correlator, i.e., the order α_s radiative corrections to the Wilson coefficients associated with the dimension-5 quark-gluon mixed condensate, and the power corrections due to the dimension-6 vacuum condensates. Combining with the similar NLO-level calculation for the decay-constant sum rule which is consistent with the precise result from recent lattice QCD calculations, we have constructed the Borel sum rules for $\lambda_{E,H}^2$. We have found that the new order- α_s radiative corrections significantly reduce the values of $\lambda_{E,H}^2$, and also make the corresponding sum rule formulas for $\lambda_{E,H}^2$ obey the correct renormalization-group equations. The resummation of the relevant logarithms of the b -quark mass based on the renormalization group has been performed and proves to improve the stability of the corresponding Borel sum rules. Our final results are obtained as Eq.(80), where the perturbative as well as nonperturbative corrections are under control and the various sources of errors are taken into account.

Compared with the previous estimate, Eq.(6), obtained in [23], the central values of our results (80) are smaller by 1/3 and the errors are also reduced considerably. On the other hand, the upper bounds of our results (80) are close to the lower bounds of Eq.(6). Study of the B -meson light-cone distribution amplitudes using the new results in the present paper will be presented elsewhere.

Acknowledgments

This work was supported by the Grant-in-Aid for Scientific Research No. B-19340063. The work of K.T. was supported in part by the Grant-in-Aid for Scientific Research on Priority Areas No. 22011012 and the Grant-in-Aid for Scientific Research Nos. 23540292, 24540284 and 25610058.

Appendix A: One-loop renormalization of dimension-5 heavy-light operators

In this Appendix, we calculate the one-loop corrections for the quark-gluon current operator arising in Eq.(8),

$$\bar{q}gG_{\mu\nu}\Gamma_1 h_v,\tag{A1}$$

in the HQET in $D = 4 + 2\epsilon$ dimensions, and determine the corresponding renormalization constants in the $\overline{\text{MS}}$ scheme. Based on this result, we also write down the explicit formula implied by the ellipses in the counter-term contribution (48).

In Eq.(A1), Γ_1 is an arbitrary gamma matrix, and μ, ν are the free Lorentz indices. The relevant one-loop diagrams are shown in Fig. 20, and those loop corrections for the operator (A1) induce the mixing with the dimension-5 heavy-light operators having the same Lorentz-transformation property as that of Eq.(A1). The corresponding mixing matrix can be obtained, in principle, by calculating only the one-particle irreducible diagrams (a)-(h) in Fig. 20, but it is

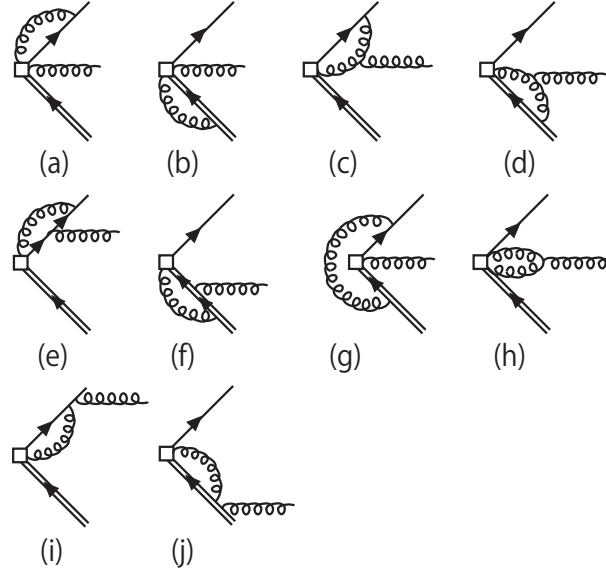


FIG. 20: The Feynman diagrams relevant for the one-loop renormalization of the quark-gluon three-body operator (A1).

known, for the case of the higher dimensional operators like Eq.(A1), that such procedure requires to treat explicitly the additional mixing of the operators that would vanish by the use of the equations of motion [33]; in particular, this implies that we have to use the off-shell external fields which, in turn, allow the mixing of the gauge-noninvariant operators as well as the gauge-invariant ones, via the corresponding one-particle irreducible diagrams, as demonstrated in many works [34] for the case of the renormalization of the higher twist operators relevant to the nucleon structure functions.

Here, to avoid such complication associated with the mixing of those “alien” operators, we calculate the relevant one-particle-reducible diagrams (i), (j) in Fig. 20 as well, so that we can adopt the usual background field method, as in the calculations of the correlators discussed in the main text; then, we may use the equations of motion for the external fields at any step of calculation [35] and the contribution from each diagram of Fig. 20 is obtained in a gauge-invariant form expressed solely in terms of the (many) three-body operators of the similar type as Eq.(A1). We use the building blocks (21), (23), (30), etc., and carry out the loop integrations in the coordinate space. The contributions of the diagrams (f) and (j) in Fig. 20 vanish because these diagrams contain the vanishing subdiagrams (a) and (b) in Fig. 2, respectively. Also, the diagrams (a) and (b) in Fig. 20 vanish by the reason similar as the diagrams in Fig. 13. The sum of the UV poles from all the other diagrams in Fig. 20 reads,

$$\begin{aligned}
& \frac{\alpha_s}{4\pi\epsilon} \left(-\frac{N_c}{8} [\bar{q}gG_{\mu\nu}\Gamma_1 h_v + 3i\bar{q}gG_{\mu\rho}\sigma_\nu{}^\rho\Gamma_1 h_v] \right. \\
& \quad - \frac{N_c}{2} \bar{q}gG_{\mu\rho}v^\rho v_\nu\Gamma_1 h_v \\
& \quad + \frac{i}{32N_c} \bar{q}gG^{\rho\lambda}\gamma_\mu [\gamma_\nu\sigma_{\rho\lambda} + \sigma_{\rho\lambda}\gamma_\nu]\Gamma_1 h_v \\
& \quad + \left[\frac{1}{4N_c} + N_c \right] \bar{q}gG_{\mu\nu}\Gamma_1 h_v \\
& \quad + \frac{C_F}{24} [2\bar{q}gG_{\mu\nu}\Gamma_1 h_v + \bar{q}gG \cdot \sigma\sigma_{\mu\nu}\Gamma_1 h_v \\
& \quad \quad \quad + 2i\bar{q}gG_{\mu\rho}\sigma_\nu{}^\rho\Gamma_1 h_v] \\
& \quad \left. - (\mu \leftrightarrow \nu), \right) \tag{A2}
\end{aligned}$$

with the last line indicating that all the preceding terms have to be antisymmetrized under the interchange $\mu \leftrightarrow \nu$. Here, the first three lines correspond to the contributions of the diagrams (c), (d), and (e) in Fig. 20, the fourth line corresponds to the diagrams (g) and (h), and the fifth and sixth lines correspond to the diagram (i).

Now, the counter-term contribution for the renormalization of the operator (A1) should be combined with Eq.(A2), so as to cancel all the UV poles arising in Eq.(A2). Thus, the corresponding counter-term contribution is given by the minus of Eq.(A2) with the replacement, $1/\epsilon \rightarrow 1/\hat{\epsilon} (= 1/\epsilon + \gamma_E - \ln 4\pi)$, in the $\overline{\text{MS}}$ scheme. Substituting this counter-term contribution for the quark-gluon current (A1) into Eq.(8) and evaluating the corresponding correlator

in D dimensions under the background fields, we immediately find that the formula implied by the ellipses in Eq.(48) is formally given by Eq.(45) with $\bar{q}(0)gG_{\mu\nu}(0)$ replaced by the minus of Eq.(A2) with $h_v \rightarrow 1$, $\epsilon \rightarrow \hat{\epsilon}$, and reads, using $\hat{\Pi}_{3H}^{\text{tree}}(\omega)$ of Eq.(46),

$$\begin{aligned}
& \frac{\alpha_s}{8\pi\hat{\epsilon}} \text{Tr} \left[\left\{ -\frac{N_c}{8} (\sigma_{\mu\nu} + 3i\sigma_{\mu\rho}\sigma_{\nu}{}^\rho) \right. \right. \\
& \quad - \frac{N_c}{2} \sigma_{\mu\rho} v^\rho v_\nu \\
& \quad + \frac{1}{32N_c} i\sigma^{\rho\lambda} \gamma_\mu (\gamma_\nu \sigma_{\rho\lambda} + \sigma_{\rho\lambda} \gamma_\nu) \\
& \quad + \left(\frac{1}{4N_c} + N_c \right) \sigma_{\mu\nu} \\
& \quad \left. + \frac{C_F}{24} (2\sigma_{\mu\nu} + (\sigma_{\rho\lambda})^2 \sigma_{\mu\nu} + 2i\sigma_{\mu\rho}\sigma_{\nu}{}^\rho) \right\} \Gamma_1 P_+ \Gamma_2 \Big] \hat{\Pi}_{3H}^{\text{tree}}(\omega) \\
& - (\mu \leftrightarrow \nu), \\
& = \frac{\alpha_s}{8\pi} \left\{ \left(\frac{1}{\hat{\epsilon}} \left[N_c - \frac{1}{2N_c} \right] - \frac{3N_c}{4} - \frac{1}{2N_c} \right) \text{Tr} [\sigma_{\mu\nu} \Gamma_1 P_+ \Gamma_2] \right. \\
& \quad \left. + \frac{N_c}{2\hat{\epsilon}} \text{Tr} [(iv_\mu \gamma_\nu - iv_\nu \gamma_\mu) \Gamma_1 P_+ \Gamma_2] \right\} \hat{\Pi}_{3H}^{\text{tree}}(\omega), \tag{A3}
\end{aligned}$$

where the final form in the RHS is presented up to the irrelevant terms that vanish as $\epsilon \rightarrow 0$.

It is worth mentioning that the results based on Eq.(A2) with the particular choices, $\Gamma_1 = \sigma^{\mu\nu} \gamma_5$ and $\Gamma_1 = \gamma^\mu \gamma_5 v^\nu$, reproduce the one-loop renormalization mixing matrix between the two pseudoscalar operators, $\bar{q}gG \cdot \sigma \gamma_5 h_v$ and $\bar{q}gG_{\mu\nu} \gamma^\mu v^\nu \gamma_5 h_v$, calculated in [36]. In particular, it is straightforward to see that the matrix elements of a system of the corresponding operator-mixing formulas yield the one-loop renormalization group equations for $\lambda_{E,H}^2$ of Eqs. (4), (5), as [36]

$$\mu \frac{d}{d\mu} \begin{pmatrix} \lambda_E^2(\mu) \\ \lambda_H^2(\mu) \end{pmatrix} + \frac{\alpha_s(\mu)}{4\pi} \hat{\gamma}_0 \begin{pmatrix} \lambda_E^2(\mu) \\ \lambda_H^2(\mu) \end{pmatrix} = 0, \tag{A4}$$

with the mixing matrix,

$$\hat{\gamma}_0 = \begin{pmatrix} \frac{8}{3}C_F + \frac{3}{2}N_c & \frac{4}{3}C_F - \frac{3}{2}N_c \\ \frac{4}{3}C_F - \frac{3}{2}N_c & \frac{8}{3}C_F + \frac{5}{2}N_c \end{pmatrix}. \tag{A5}$$

Finally, we mention that the one-loop renormalization of the operator (47) to obtain the renormalization constant (56) can be carried out in a similar manner as above. Indeed, most results can be obtained from the above result (A2) by the formal substitutions, $h_v \rightarrow q$ and $\Gamma_1 \rightarrow \sigma_{\mu\nu}$, for an external quark field and the gamma matrix structure, respectively, and thus need not new calculation. The only diagram that requires new calculation is the one corresponding to the diagram (g) in Fig. 20. We have only one flavor-singlet, scalar three-body operator of dimension-5, given by Eq.(47), and thus do not encounter the operator mixing in the background field method for this case.

Appendix B: Quark-gluon three-body components in the π and K mesons

In this Appendix, we compare our estimate (80) of the quark-gluon three-body components in the B meson with the values of the corresponding quantities of light pseudoscalar mesons, π , K . For definiteness, we will give most of the following discussions for the case of K mesons, i.e., $s\bar{q}$ bound states with $q = u, d$. The K -meson matrix elements of three-body local operators of dimension 5 in QCD read

$$\langle 0 | \bar{q} \gamma_\alpha g \tilde{G}_{\rho\sigma} s | K(p) \rangle = \frac{i}{3} f_K \delta_K^2 (g_{\alpha\sigma} p_\rho - g_{\alpha\rho} p_\sigma), \tag{B1}$$

$$\langle 0 | \bar{q} \gamma_\alpha \gamma_5 i g G_{\rho\sigma} s | K(p) \rangle = \frac{i}{3} f_K m_K^2 \kappa_{4K} (g_{\alpha\sigma} p_\rho - g_{\alpha\rho} p_\sigma), \tag{B2}$$

$$\langle 0 | \bar{q} \sigma_{\alpha\beta} \gamma_5 g G_{\mu\nu} s | K(p) \rangle = i f_{3K} [p_\beta (g_{\alpha\mu} p_\nu - g_{\alpha\nu} p_\mu) - p_\alpha (g_{\beta\mu} p_\nu - g_{\beta\nu} p_\mu)] + i m_K^2 \varphi_K (g_{\alpha\mu} g_{\beta\nu} - g_{\alpha\nu} g_{\beta\mu}), \tag{B3}$$

where $\tilde{G}_{\rho\sigma} = \frac{1}{2}\epsilon_{\rho\sigma\xi\eta}G^{\xi\eta}$, $|K(p)\rangle$ is the kaon state with the 4-momentum p , obeying $\langle K(p)|K(p')\rangle = 2p^0(2\pi)^3\delta^{(3)}(p-p')$ and $p^2 = m_K^2$, and f_K denotes the decay constant, as usual,

$$\langle 0|\bar{q}\gamma_\rho\gamma_5 s|K(p)\rangle = if_K p_\rho. \quad (\text{B4})$$

We follow the notation of Ref.[37] for the nonperturbative parameters f_{3K} , δ_K^2 , and κ_{4K} ; f_{3K} corresponds to twist-3 and δ_K^2 , κ_{4K} correspond to twist-4. Here, we also need to deal explicitly with φ_K , which corresponds to twist-5. The matrix elements of $\bar{q}Gs$ operators associated with the Dirac matrices other than those in Eqs. (B1)-(B3) vanish. Thus, the meson matrix elements of the dimension-5 three-body operators in QCD are expressed by the four independent nonperturbative parameters; compare with the corresponding B -meson matrix element (12) expressed by the two independent parameters $\lambda_{E,H}^2$. In the rest frame, Eqs. (B1)-(B3) yield the matrix elements associated with the chromoelectric and chromomagnetic fields, as

$$\begin{aligned} \langle 0|\bar{q}\boldsymbol{\alpha} \cdot g\mathbf{E}\gamma_5\gamma_0 s|K(p)\rangle &= -m_K^3 f_K \kappa_{4K}, \\ \langle 0|\bar{q}\boldsymbol{\sigma} \cdot g\mathbf{H}\gamma_5\gamma_0 s|K(p)\rangle &= im_K f_K \delta_K^2, \\ \langle 0|\bar{q}\boldsymbol{\alpha} \cdot g\mathbf{E}\gamma_5 s|K(p)\rangle &= -3m_K^2 (f_{3K} + \varphi_K), \\ \langle 0|\bar{q}\boldsymbol{\sigma} \cdot g\mathbf{H}\gamma_5 s|K(p)\rangle &= -3im_K^2 \varphi_K, \end{aligned} \quad (\text{B5})$$

with $p = (m_K, \mathbf{0})$, and, using Eq.(B4), the ratios independent of the normalization of the meson state read,

$$\frac{i\langle 0|\bar{q}\boldsymbol{\alpha} \cdot g\mathbf{E}\gamma_5\gamma_0 s|K(p)\rangle}{\langle 0|\bar{q}\gamma_0\gamma_5 s|K(p)\rangle} = -m_K^2 \kappa_{4K}, \quad (\text{B6})$$

$$\frac{\langle 0|\bar{q}\boldsymbol{\sigma} \cdot g\mathbf{H}\gamma_5\gamma_0 s|K(p)\rangle}{\langle 0|\bar{q}\gamma_0\gamma_5 s|K(p)\rangle} = \delta_K^2, \quad (\text{B7})$$

$$\frac{\langle 0|\bar{q}\boldsymbol{\sigma} \cdot g\mathbf{H}\gamma_5 s|K(p)\rangle - i\langle 0|\bar{q}\boldsymbol{\alpha} \cdot g\mathbf{E}\gamma_5 s|K(p)\rangle}{\langle 0|\bar{q}\gamma_0\gamma_5 s|K(p)\rangle} = 3m_K \frac{f_{3K}}{f_K}, \quad (\text{B8})$$

where the last formula is obtained by eliminating the twist-5 quantity φ_K , whose value is unknown. On the other hand, using Eqs. (1), (4) and (5), we have the similar ratios for the B -meson at rest:

$$\frac{i\langle 0|\bar{q}\boldsymbol{\alpha} \cdot g\mathbf{E}\gamma_5 h_v|\bar{B}(v)\rangle}{\langle 0|\bar{q}\gamma_0\gamma_5 h_v|\bar{B}(v)\rangle} = \lambda_E^2, \quad (\text{B9})$$

$$\frac{\langle 0|\bar{q}\boldsymbol{\sigma} \cdot g\mathbf{H}\gamma_5 h_v|\bar{B}(v)\rangle}{\langle 0|\bar{q}\gamma_0\gamma_5 h_v|\bar{B}(v)\rangle} = \lambda_H^2. \quad (\text{B10})$$

Therefore, the value of $\lambda_H^2 - \lambda_E^2$ may be compared with that of Eq.(B8). The use of $h_v = \not{p}h_v = \gamma_0 h_v$ in the rest frame would suggest another (rough) comparison of Eqs.(B9) and (B10), respectively, with Eqs.(B6) and (B7).

In Ref.[37], numerical values of the nonperturbative parameters δ_K^2 , κ_{4K} and f_{3K} and the similar quantities for the pion are evaluated from QCD sum rules, using the QCD correlation functions analogous to the HQET correlators treated in this paper [40]. The values presented in Ref.[37] are

$$\begin{aligned} \delta_\pi^2 &= 0.18 \pm 0.06 \text{ GeV}^2, & \kappa_{4\pi} &= 0, & f_{3\pi} &= 0.0045 \pm 0.0015 \text{ GeV}^2, \\ \delta_K^2 &= 0.20 \pm 0.06 \text{ GeV}^2, & \kappa_{4K} &= -0.09 \pm 0.02, & f_{3K} &= 0.0045 \pm 0.0015 \text{ GeV}^2, \end{aligned} \quad (\text{B11})$$

for the π as well as K meson, where all values are given at the scale $\mu = 1 \text{ GeV}$. Note that the G-parity-breaking contribution (B2) vanishes for the pion case. Combined with $m_\pi = 140 \text{ MeV}$, $m_K = 494 \text{ MeV}$, $f_\pi = 131 \text{ MeV}$, and $f_K = 160 \text{ MeV}$, we obtain the values of Eqs. (B6)-(B8):

$$\begin{aligned} \frac{\langle 0|\bar{q}\boldsymbol{\sigma} \cdot g\mathbf{H}\gamma_5 s|K(p)\rangle - i\langle 0|\bar{q}\boldsymbol{\alpha} \cdot g\mathbf{E}\gamma_5 s|K(p)\rangle}{\langle 0|\bar{q}\gamma_0\gamma_5 s|K(p)\rangle} &= 0.042 \pm 0.014 \text{ GeV}^2, \\ \frac{i\langle 0|\bar{q}\boldsymbol{\alpha} \cdot g\mathbf{E}\gamma_5\gamma_0 s|K(p)\rangle}{\langle 0|\bar{q}\gamma_0\gamma_5 s|K(p)\rangle} &= 0.022 \pm 0.005 \text{ GeV}^2, & \frac{\langle 0|\bar{q}\boldsymbol{\sigma} \cdot g\mathbf{H}\gamma_5\gamma_0 s|K(p)\rangle}{\langle 0|\bar{q}\gamma_0\gamma_5 s|K(p)\rangle} &= 0.20 \pm 0.06 \text{ GeV}^2, \end{aligned} \quad (\text{B12})$$

which may be compared with our values of $\lambda_H^2 - \lambda_E^2$, λ_E^2 , and λ_H^2 , respectively, see Eq.(80). For the pion, we obtain similarly,

$$\begin{aligned} \frac{\langle 0|\bar{q}\boldsymbol{\sigma} \cdot g\mathbf{H}\gamma_5 s|\pi(p)\rangle - i\langle 0|\bar{q}\boldsymbol{\alpha} \cdot g\mathbf{E}\gamma_5 s|\pi(p)\rangle}{\langle 0|\bar{q}\gamma_0\gamma_5 s|\pi(p)\rangle} &= 0.014 \pm 0.005 \text{ GeV}^2, \\ \frac{i\langle 0|\bar{q}\boldsymbol{\alpha} \cdot g\mathbf{E}\gamma_5\gamma_0 s|\pi(p)\rangle}{\langle 0|\bar{q}\gamma_0\gamma_5 s|\pi(p)\rangle} &= 0, & \frac{\langle 0|\bar{q}\boldsymbol{\sigma} \cdot g\mathbf{H}\gamma_5\gamma_0 s|\pi(p)\rangle}{\langle 0|\bar{q}\gamma_0\gamma_5 s|\pi(p)\rangle} &= 0.18 \pm 0.06 \text{ GeV}^2. \end{aligned} \quad (\text{B13})$$

Thus, the quark-antiquark-gluon three-body components are different between the B meson and the light π, K mesons, but the present results suggest that their orders of magnitude are not largely different. In particular, the “splitting” between the chromomagnetic and chromoelectric fields, $\lambda_H^2 - \lambda_E^2$, has similar size as the first quantity in Eqs.(B12) and (B13). In this connection, it is worth mentioning the following: the dimension-5 quark-gluon mixed condensates arise accompanying a quark mass, as $m_q \langle \bar{q}gG \cdot \sigma q \rangle$, $m_s \langle \bar{q}gG \cdot \sigma q \rangle$, etc., in the OPE in full QCD to derive the sum rules in Ref.[37], so that the mixed condensates play minor role near the chiral limit. On the other hand, the quark-gluon mixed condensates give a dominant contribution in the heavy-quark limit for the B -meson case, as demonstrated in this paper, but the splitting $\lambda_H^2 - \lambda_E^2$ receives the contribution of the mixed condensates at $O(\alpha_s)$, see Eq.(62).

-
- [1] M. Antonelli *et al.*, Phys. Rept. **494**, 197 (2010).
 - [2] M. Neubert, Phys. Rept. **245**, 259 (1994).
 - [3] E. Gamiz, C. T. H. Davies, G. P. Lepage, J. Shigemitsu and M. Wingate [HPQCD Collaboration], Phys. Rev. **D80**, 014503 (2009).
 - [4] C. Bernard *et al.*, PoS **LATTICE2008**, 278 (2008); A. Bazavov *et al.* [Fermilab Lattice and MILC Collaborations], Phys. Rev. **D85**, 114506 (2012).
 - [5] B. Blossier *et al.* [ETM Collaboration], JHEP **1004**, 049 (2010).
 - [6] A. J. Schwartz, AIP Conf. Proc. **1182**, 299 (2009).
 - [7] K. Ikado *et al.* [Belle Collaboration], Phys. Rev. Lett. **97**, 251802 (2006); K. Hara *et al.* [Belle Collaboration], Phys. Rev. **D82**, 071101 (2010); I. Adachi *et al.* [Belle Collaboration], Phys. Rev. Lett. **110**, 131801 (2013).
 - [8] B. Aubert *et al.* [BABAR Collaboration], Phys. Rev. **D76**, 052002 (2007); P. del Amo Sanchez *et al.* [BaBar Collaboration], arXiv:1008.0104 [hep-ex]; B. Aubert *et al.* [BaBar Collaboration], Phys. Rev. D **81**, 051101 (2010).
 - [9] A. G. Grozin and M. Neubert, Phys. Rev. **D55**, 272 (1997).
 - [10] E. Bagan, P. Ball, V. M. Braun and H. G. Dosch, Phys. Lett. **B278**, 457 (1992).
 - [11] A. A. Penin and M. Steinhauser, Phys. Rev. **D65**, 054006 (2002).
 - [12] A. R. Zhitnitsky, I. R. Zhitnitsky and V. L. Chernyak, Sov. J. Nucl. Phys. **41**, 284 (1985) [Yad. Fiz. **41**, 445 (1985)]; V. M. Braun and I. E. Filyanov, Z. Phys. **C48**, 239 (1990); P. Ball, V. M. Braun, Y. Koike and K. Tanaka, Nucl. Phys. **B529**, 323 (1998).
 - [13] H. Kawamura, J. Kodaira, C.F. Qiao and K. Tanaka, Phys. Lett. **B523**, 111 (2001); Erratum-ibid. **B536**, 344 (2002); Mod. Phys. Lett. **A18**, 799 (2003); Nucl. Phys. B (Proc. Suppl.) **116**, 269 (2003); H. Kawamura, J. Kodaira and K. Tanaka, Prog. Theor. Phys. **113**, 183 (2005).
 - [14] T. Huang, X. G. Wu and M. Z. Zhou, Phys. Lett. **B611**, 260 (2005); B. Geyer and O. Witzel, Phys. Rev. **D72**, 034023 (2005); T. Huang, C. F. Qiao and X. G. Wu, Phys. Rev. **D73**, 074004 (2006); B. Geyer and O. Witzel, Phys. Rev. **D76**, 074022 (2007); A. Khodjamirian, T. Mannel and N. Offen, Phys. Lett. **B620**, 52 (2005); A. Khodjamirian, T. Mannel and N. Offen, Phys. Rev. **D75**, 054013 (2007); A. Le Yaouanc, L. Oliver and J. C. Raynal, Phys. Rev. **D77**, 034005 (2008).
 - [15] V. M. Braun, D. Y. Ivanov and G. P. Korchemsky, Phys. Rev. **D69**, 034014 (2004).
 - [16] S. J. Lee and M. Neubert, Phys. Rev. **D72**, 094028 (2005).
 - [17] S. Descotes-Genon and N. Offen, JHEP **0905**, 091 (2009); M. Knodlseder and N. Offen, JHEP **1110**, 069 (2011).
 - [18] H. Kawamura and K. Tanaka, Phys. Lett. **B673**, 201 (2009); H. Kawamura and K. Tanaka, Phys. Rev. **D81**, 114009 (2010).
 - [19] G. Bell and V. Pilipp, Phys. Rev. **D80**, 054024 (2009); M. Beneke, T. Huber and X. Q. Li, Nucl. Phys. **B832**, 109 (2010).
 - [20] E. V. Shuryak, Nucl. Phys. **B198**, 83 (1982).
 - [21] M. Neubert, Phys. Rev. **D45**, 2451 (1992).
 - [22] V. A. Novikov, M. A. Shifman, A. I. Vainshtein and V. I. Zakharov, Fortsch. Phys. **32**, 585 (1984).
 - [23] See, e.g., A. G. Grozin, Int. J. Mod. Phys. **A10**, 3497 (1995).
 - [24] L. F. Abbott, Nucl. Phys. **B185**, 189 (1981); Acta Phys. Polon. **B13**, 33 (1982).
 - [25] S. Narison and R. Tarrach, Phys. Lett. **B125**, 217 (1983).
 - [26] A. Y. Morozov, Sov. J. Nucl. Phys. **40**, 505 (1984); Preprints ITEP-190, 191 (1983).
 - [27] X. -D. Ji and M. J. Musolf, Phys. Lett. **B257**, 409 (1991); D. J. Broadhurst and A. G. Grozin, Phys. Lett. **B267**, 105 (1991).
 - [28] D. J. Broadhurst and A. G. Grozin, Phys. Lett. **B274**, 421 (1992).
 - [29] S. Narison, Camb. Monogr. Part. Phys. Nucl. Phys. Cosmol. **17**, 1 (2002).
 - [30] P. Ball and V. M. Braun, Phys. Rev. D **49**, 2472 (1994) [hep-ph/9307291].
 - [31] M. Neubert, Phys. Rev. **D46**, 1076 (1992).
 - [32] K. Nakamura *et al.* [Particle Data Group], J. Phys. G **37**, 075021 (2010).
 - [33] H. D. Politzer, Nucl. Phys. **B172**, 349 (1980); J. C. Collins, *Renormalization*, (Cambridge University Press, 1984); J. Kodaira and K. Tanaka, Prog. Theor. Phys. **101**, 191 (1999).
 - [34] J. Kodaira, Y. Yasui and T. Uematsu, Phys. Lett. **B344**, 348 (1995); J. Kodaira, Y. Yasui, K. Tanaka and T. Uematsu, Phys. Lett. **B387**, 855 (1996); Y. Koike and K. Tanaka, Phys. Rev. **D51**, 6125 (1995); Y. Koike and N. Nishiyama, Phys. Rev. **D55**, 3068 (1997); H. Kawamura, T. Uematsu, J. Kodaira and Y. Yasui, Mod. Phys. Lett. **A12**, 135 (1997); H. Kawamura, Z. Phys. **C75**, 27 (1997).

- [35] E. V. Shuryak and A. I. Vainshtein, Nucl. Phys. **B199**, 451 (1982); **B201**, 141 (1982); A. P. Bukhvostov, E. A. Kuraev and L. N. Lipatov, Sov. Phys. JETP **60**, 22 (1984); I. I. Balitsky and V. M. Braun, Nucl. Phys. **B311**, 541 (1989); J. Kodaira, T. Nasuno, H. Tochimura, K. Tanaka and Y. Yasui, Prog. Theor. Phys. **99**, 315 (1998).
- [36] A. G. Grozin and M. Neubert, Nucl. Phys. **B495**, 81 (1997).
- [37] P. Ball, V. M. Braun and A. Lenz, JHEP **0605**, 004 (2006).
- [38] $\gamma_{\sigma 0}$ has been obtained in Ref. [25] and, independently and simultaneously, in Ref. [26]. γ_{J1} is obtained in Ref. [27]. See also Refs. [2, 29].
- [39] The sum rule analysis of the value of $\bar{\Lambda}$, calculating the ratio of Eq.(79) and its first derivative with respect to $1/M$ [10, 31], does not serve to reduce further the range of the values of $\bar{\Lambda}$ nor ω_{th} for the present case: the corresponding derivative of Eq.(79) would receive the large $O(\alpha_s^2)$ perturbative corrections for small M [2, 21] while it appears to be dominated by higher resonances and continuum contributions for moderate as well as large M ; such behaviors are pronounced with the present use of $\alpha_s(1 \text{ GeV}) \simeq 0.47$ which is larger than the value of α_s in the literature [10, 31].
- [40] Estimate of the nonperturbative parameters in Ref.[37] is performed using not only the correlators between the two- and three-body currents but also those between the two three-body currents.